To the Graduate Council:

I am submitting herewith a thesis written by Eugenia Beth Lee entitled "Accident Dosimetry Using Panasonic Dosimeters." I have examined the final copy of this thesis for form and content and recommend that it be accepted in partial fulfillment of the requirements for the degree of Master of Science, with a major in Nuclear Engineering.

Laurence F. Miller

Laurence F. Miller, Major Professor

We have read this thesis
and recommend its acceptance:

Accepted for the Council:

Associate Vice Chancellor
and Dean of The Graduate School

STATEMENT OF PERMISSION TO USE

In presenting this thesis in partial fulfillment of the requirements for a Master's degree at The University of Tennessee, Knoxville, I agree that the Library shall make it available to borrowers under rules of the Library. Brief quotations are allowable without special permission, provided that accurate acknowledgment of the source is made.

Permission for extensive quotation from or reproduction of this thesis may be granted by my major, or in his absence, by the Head of the Interlibrary Services when, in the opinion of either, the proposed use of the material is for scholarly purposes. Any copying or use of the material in this thesis for financial gain shall not be allowed without my written permission.

Signature Eugenia Ruth Lee

Date December 2, 1994

ACCIDENT DOSIMETRY USING PANASONIC DOSIMETERS

A Thesis

Presented for the

Master of Science

Degree

The University of Tennessee, Knoxville

Eugenia Beth Lee

December 1994

DEDICATION

This thesis is dedicated to my parents, Wanda and Eugene Lee, and my sister, Kara Lee, for their encouragement and for never doubting my abilities even when I did. This thesis is also dedicated to Joel McDuffee, my husband, whose constant aide and encouragement made this thesis a reality.

ACKNOWLEDGEMENTS

I would like to acknowledge Panasonic Industrial Company for their financial support on this project. In particular, I would like to thank Dave Katzman, Paul Wasek, and John Lazur for their help and guidance. I would also like to thank my research advisors: Bill Casson and Larry Miller, my major professor, for their constant guidance, patience, and encouragement. I would also like to recognize my other committee members: Peter Groer and Dave Simpson. I would like to acknowledge ORNL's Health Science Research Division for providing support and for allowing me to use RADCAL. I would like to thank RADCAL's facility manager, Jim Bogard, for his encouragement and guidance on this project and RADCAL's facility operator, Bill Robbins, for spending a great deal of time and effort in aiding my exposures. I would also like to recognize Sue Roddy and her staff at TVA Watt's Bar facility for graciously allowing me to use their reader. I would also like to recognize my family and friends whose constant encouragement throughout the years has enabled the completion of this work.

ABSTRACT

Criticality accident personnel dosimetry involves the evaluation of high doses in mixed fields of gamma rays and neutrons. Those who work in areas where there is potential for a criticality accident or other extremely high neutron doses need dosimeters, such as thermoluminescent dosimeters, capable of measuring doses associated with these scenarios. In order for a dosimeter to be used in these areas, it must be characterized for accident or high level neutron dosimetry. Panasonic thermoluminescent dosimeters (TLDs), using lithium tetraborate, have been characterized for accident and high level neutron dosimetry.

The characterization of these dosimeters includes calculating the dosimeter's response to neutrons, determining the dosimeter's response to various possible accident scenarios, and evaluating TLD's response at high doses.

An accurate determination of neutron dose is complicated by the fact that dose per source neutron is a strong function of energy. Correction factors for dose and for the dosimeter's response are obtained for 115 different spectra, and these effects are incorporated into a single spectral correction factor (SCF) for each spectrum. These SCFs should be improved, however, to correct for neutrons scattered from the body. Also, a linear combination of element responses to bare, D_2O-moderated, and polyethylene-moderated californium-252 and americium-241/beryllium are used to obtain some spectral information from any unknown spectrum.

Since accident dosimetry involves extremely high doses, the element responses have been tested for linearity from one to one thousand rad with D_2O-moderated ^{252}Cf. Corrections for element responses due to doses above ten rad have been determined.

Results from this study demonstrate that Panasonic dosimeters, using lithium tetraborate, can be used by personnel who work in areas where there is a possibility for a criticality accident.

TABLE OF CONTENTS

I. INTRODUCTION 1

II. THEORY 3

2.1. Thermoluminescent Mechanism 3

2.2. Energy Deposition of Lithium Tetraborate 8

2.3. Integral Thermoluminescence 18

2.4. Response of $Li_2B_4O_7$ to Possible Accident Scenarios 21

2.5. Element Correction Factor 35

2.5.1. Step 1: Irradiate Reference Dosimeters 35

2.5.2. Step 2: Calculate Reference Means for Reference Group . . 36

2.5.3. Step 3: Produce ECFs Based on Element Means 36

2.5.4. Step 4: Repeat Steps 1 through 3 36

2.5.5. Step 5: Average the ECFs for Each Element 37

2.5.6. Step 6: Examine ECFs and %CVs of Reference Group . . . 37

2.5.7. Step 7: Irradiate Non-reference Dosimeters 37

2.5.8. Step 8: Calculate Element Means of Reference Set 37

2.5.9. Step 9: Produce ECFs for Non-reference Dosimeters 40

2.5.10. Step 10: Examine ECFs of Non-reference Dosimeters . . . 40

2.6. Supralinearity 41

2.7 Response Function Using Four Neutron Spectra 42

III. EQUIPMENT AND MATERIALS 46

3.1. RADCAL 46

3.2. Sources 47
3.2.1. Amersham Beam Irradiator 47
3.2.2. J. L. SHEPHERD Panoramic Irradiator 48
3.2.3. Neutron Sources 48
3.3. Panasonic UD-702E Reader 50
3.4. Panasonic UD-710E Reader 52
3.5. Panasonic UD-809AS 52
3.6. Panasonic UD-802AS 55
3.7. PMMA Phantom 55

IV. RESULTS 57
4.1 Supralinearity 57
4.2 Response Function Using Four Neutron Spectra 58
4.3 Effects of Phantom 62

V. CONCLUSIONS AND FUTURE WORK 66

BIBLIOGRAPHY 67

APPENDICES 75
A. DATA 76
A.1 Data from ECF Exposures 76
A.2 Data for Neutron and Gamma Equivalence 91
A.3 Data for Response Function Using Four Neutron Spectra . . . 93
A.4 Data for Supralinearity Measurements 101

A.5 Data for Phantom Effects 119

B. VENDOR'S ADDRESSES AND TELEPHONE NUMBERS . . . 122

C. RESPONSE OF $^{6}Li_{2}{}^{10}B_{4}O_{7}$ TO ROOM SCATTER 123

VITA 137

LIST OF TABLES

Table 2.1 Values for A, α, and ε for Lithium, Boron, and Oxygen. 13

Table 2.2 Interactions Along with Q Values Used in the Calculation of Kerma Per Unit Fluence for $^{6}Li_{2}{}^{10}B_{4}O_{7}$ 14

Table 2.3 Interactions Along with Q Values Used in the Calculation of Kerma Per Unit Fluence for $^{7}Li_{2}{}^{11}B_{4}O_{7}$ 16

Table 2.4 Overall Conversion Efficiency, $\eta(\lambda)$, from Kerma to Integral Thermoluminescence for Panasonic's UD-809AS. 19

Table 2.5 Accident Scenarios with Doses, Response of UD-809AS, and SCFs. . . . 23

Table 2.6 Reference Group Average ECFs and Standard Deviations 38

Table 2.7 Energy Groups and Ranges for Response Function Using Four Neutron Spectra. 44

Table 3.1 Calibration Information on Neutron Sources 49

Table 3.2 Thermal Cross-sections and Natural Abundances of Lithium and Boron . 54

Table 4.1 Results of Supralinearity Measurements for the UD-809AS Dosimeters. 61

Table 4.2 Results of Supralinearity Measurements for the UD-802AS Dosimeters. 61

Table 4.3 Coefficients for Determining Fluence for Each Energy Group. 63

Table 4.4 Fractional Fluence for Energy Bins for ^{238}Pu-Be. 63

Table 4.5 Phantom Correction Factors for Panasonic UD-809AS. 65

Table 4.6 Phantom Correction Factors for Panasonic UD-802AS. 65

Table A.1.1 TLD Readings in Units of mR* for Reference Group Exposed to 500 mR of Cesium-137 for ECF Calculation. 76

Table A.1.2 TLD Readings in Units of mR* for Reference Group Exposed to 500 mR of Cesium-137 for ECF Calculation. 78

Table A.1.3 TLD Readings in Units of mR* for Reference Group Exposed to 500 mR of Cesium-137 for ECF Calculation. 80

Table A.1.4 TLD Readings in Units of mR* for Non-Reference Group Exposed to 500 mR of Cesium-137 for ECF Calculation 82

Table A.1.5 TLD Readings in Units of mR* for Reference Sub-Group Exposed to 500 mR of Cesium-137 for ECF Calculation. 87

Table A.1.6 TLD Readings in Units of mR* for Non-Reference Group Exposed to 500 mR of Cesium-137 for ECF Calculation. 88

Table A.1.7 TLD Readings in Units of mR* for Reference Sub-Group Exposed to 500 mR of Cesium-137 for ECF Calculation. 89

Table A.1.8 TLD Readings in Units of mR* for Non-Reference Group Exposed to 500 mR of Cesium-137 for Justification for Using Only One Irradiation for Non-Reference ECF Calculation 90

Table A.1.9 TLD Readings in Units of mR* for Reference Sub-Group Exposed to 500 mR of Cesium-137 for Justification for Using Only One Irradiation for Non-Reference ECF Calculation 90

Table A.2.1 TLD Readings in Units of mR* for Exposure of 500 mR of Cesium-137 for Calculation of Cesium Equivalence. 91

Table A.2.2 TLD Readings in Units of mR* for 500 mrem Exposure to D_2O-Moderated Californium-252 for Calculation of D_2O Equivalence 92

Table A.3.1 TLD Readings in Units of mR* for 500 mrem Exposure to D_2O-Moderated Californium-252 for Combination of Four Sources. 93

Table A.3.2 TLD Readings in Units of mR* for 500 mrem Exposure to Bare Californium-252 for Combination of Four Sources. 95

Table A.3.3 TLD Readings in Units of mR* for 500 mrem Exposure to Americium-Beryllium for Combination of Four Sources. 97

Table A.3.4 TLD Readings in Units of mR* for 500 mrem Exposure to Polyethylene-Moderated Californium-252 for Combination of Four Sources. 99

Table A.3.5 TLD Readings in Units of mR* for 500 mrem Exposure to Plutonium-Beryllium for Verification of Combination of Four Sources Technique. . 100

Table A.4.1 TLD Readings in Units of R* for Dosimeters Exposed to 1 rem (0.097 rad) of D_2O-Moderated ^{252}Cf. 101

Table A.4.2 TLD Readings in Units of R* for Dosimeters Exposed to 2 rem (0.193 rad) of D_2O-Moderated ^{252}Cf. 103

Table A.4.3 TLD Readings in Units of R* for Dosimeters Exposed to 5 rem (0.484 rad) of D_2O-Moderated ^{252}Cf. 105

Table A.4.4 TLD Readings in Units of R* for Dosimeters Exposed to 10 rem (0.967 rad) of D_2O-Moderated ^{252}Cf. 107

Table A.4.5 TLD Readings in Units of R* for Dosimeters Exposed to 50 rem (4.84 rad) of D_2O-Moderated ^{252}Cf. 109

Table A.4.6 TLD Readings in Units of R* for Dosimeters Exposed to 100 rem (9.67 rad) of D_2O-Moderated ^{252}Cf. 111

Table A.4.7 TLD Readings in Units of R* for Dosimeters Exposed to 499 rem (48.23 rad) of D_2O-Moderated ^{252}Cf. 113

Table A.4.8 TLD Readings in Units of R* for Dosimeters Exposed to 747 rem (72.27 rad) of D_2O-Moderated ^{252}Cf. 114

Table A.4.9 TLD Readings in Units of R* for Dosimeters Exposed to 939 rem (90.80 rad) of D_2O-Moderated ^{252}Cf. 115

Table A.4.10 TLD Readings in Units of R* for Dosimeters Exposed to 5,089 rem (492.12 rad) of D_2O-Moderated ^{252}Cf. 116

Table A.4.11 TLD Readings in Units of R* for Dosimeters Exposed to 7,756 rem (750.0 rad) of D_2O-Moderated ^{252}Cf. 117

Table A.4.12 TLD Readings in Units of R* for Dosimeters Exposed to 10,611 rem (1026.09 rad) of D_2O-Moderated ^{252}Cf. 118

Table A.5.1 TLD Readings in Units of mR* for Dosimeters Exposed to 500 mrem of D_2O-Moderated ^{252}Cf at 50 cm in Air. 119

Table A.5.2 TLD Readings in Units of mR* for Dosimeters Exposed to 500 mrem of Bare ^{252}Cf at 50 cm in Air. 120

Table A.5.3 TLD Readings in Units of mR* for Dosimeters Exposed to 500 mrem of Polyethylene-Moderated ^{252}Cf at 50 cm in Air. 121

LIST OF FIGURES

Figure 2.1 Diagram Showing Both Electron and Hole Traps in a TLD Material. 5

Figure 2.2 Formation of an Electron-Hole Pair in a TLD Material When Exposed to Radiation. 6

Figure 2.3 First Possible Mode of Recombination When Heat Is Applied. 7

Figure 2.4 Second Possible Mode Recombination When Heat Is Applied. 9

Figure 2.5 Energy Deposition for $^{6}Li_{2}{}^{10}B_{4}O_{7}$ Along with the Contribution for Each Element: ^{6}Li, ^{10}B, and ^{16}O. 15

Figure 2.6 Energy Deposition for Both $^{6}Li_{2}{}^{10}B_{4}O_{7}$ and $^{7}Li_{2}{}^{11}B_{4}O_{7}$. 17

Figure 2.7 Actual Dose Versus the 809AS Response for Each Accident Scenario. 33

Figure 3.1 Optical Heating Method for the Panasonic UD-809AS (Panasonic Industrial Company, 1989). 51

Figure 3.2 Panasonic UD-809AS Thermoluminescent Dosimeter. 53

Figure 4.1 Panasonic UD-809AS Response to D_2O-Moderated ^{252}Cf. 59

Figure 4.2 Panasonic UD-802AS Response to D_2O-Moderated ^{252}Cf. 60

Figure C.1 Response of Bare Detector as a Function of Distance^2 for Bare ^{252}Cf. 126

Figure C.2 Response of Two Inch Sphere Detector as a Function of Distance^2 for Bare ^{252}Cf. 126

Figure C.3 Response of Three Inch Sphere Detector as a Function of Distance^2 for Bare ^{252}Cf. 127

Figure C.4 Response of Five Inch Sphere Detector as a Function of Distance^2 for Bare ^{252}Cf. 127

Figure C.5 Response of Eight Inch Sphere Detector as a Function of Distance^2 for Bare ^{252}Cf. 128

Figure C.6 Response of Ten Inch Sphere Detector as a Function of Distance^2 for Bare ^{252}Cf. 128

Figure C.7 Response of Twelve Inch Sphere Detector as a Function of Distance^2 for Bare ^{252}Cf. 129

Figure C.8 Response of Bare Detector as a Function of Distance^2 for D_2O-Moderated ^{252}Cf. 131

Figure C.9 Response of Two Inch Sphere Detector as a Function of Distance^2 for D_2O-Moderated ^{252}Cf. 131

Figure C.10 Response of Three Inch Sphere Detector as a Function of Distance^2 for D_2O-Moderated ^{252}Cf. 132

Figure C.11 Response of Five Inch Sphere Detector as a Function of Distance^2 for D_2O-Moderated ^{252}Cf. 132

Figure C.12 Response of Eight Inch Sphere Detector as a Function of Distance^2 for D_2O-Moderated ^{252}Cf. 133

Figure C.13 Response of Ten Inch Sphere Detector as a Function of Distance^2 for D_2O-Moderated ^{252}Cf. 133

Figure C.14 Response of Twelve Inch Sphere Detector as a Function of Distance^2 for D_2O-Moderated ^{252}Cf. 134

Figure C.15 Response of $^6Li_2{}^{10}B_4O_7$ to Direct and Room Scatter Flux for Bare ^{252}Cf. 135

Figure C.16 Response of $^6Li_2{}^{10}B_4O_7$ to Direct and Room Scatter Flux for D_2O-Moderated ^{252}Cf. 136

CHAPTER I

INTRODUCTION

Accident dosimetry is an important part of external personnel dosimetry because it is the dosimetry of personnel exposed in a nuclear criticality accident which is defined as "an unplanned or uncontrolled nuclear excursion resulting from the assembly of a quantity of fissile material" (IAEA, 1982). Accident dosimetry typically involves measuring large doses from mixed gamma and neutron fields. Accident dosimetry should be capable of measuring a gamma dose in the range from 10 to 1000 rad with an accuracy of 20% and a neutron dose in the range from 1 to 1000 rad with an accuracy of 30% (DOE 5480.11). The units used in accident dosimetry are absorbed dose (rad or grey) rather than dose equivalent (rem or sievert) because dose equivalent is a risk estimate for stochastic effects at low doses.

According to 10 CFR 835, accident dosimetry shall be provided by installations which possess "sufficient quantities of fissile material to potentially constitute a critical mass such that the excessive exposure of personnel to radiation from a nuclear accident" could occur and should include 1) biological systems, such as hair and blood activation analysis, 2) fixed nuclear accident dosimetry systems, such as wall threshold units, and 3) personnel nuclear accident dosimeters, such as film badges, indium foils, or thermoluminescent dosimeters (10 CFR 835.1304, 1994). These same installations must be capable of rapidly determining which personnel receive an absorbed dose of 10 rad or

more (10 CFR 70.24). By quickly identifying these individuals, medical attention can be directed towards the proper patients, and potential victims who are not exposed to large doses can be assured that immediate health concerns are not an issue.

A rapid and convenient method of accident dosimetry is using thermolumonescent dosimeters (TLD). Most installations that use TLDs already have all the necessary equipment, TLDs and readers, on-site for a personnel nuclear accident dosimetry system. Panasonic dosimeters, being one of the most popular TLDs on today's market, are being used by numerous companies and utilities such as: Commonwealth Edison, Yankee Atomic, and Tennessee Valley Authority. Because of the popularity and convenience of these dosimeters, Panasonic TLDs are an ideal choice for a personnel nuclear accident dosimetry system for these and many other companies. In order for Panasonic dosimeters as well as other types of dosimeters to be used in this capacity, they must be characterized for accident dosimetry in fields of high-level neutron and gamma doses. The primary purpose of this research is to characterize Panasonic dosimeters to accident dosimetry in the form of high-level neutron doses. This characterization includes the calculation of Panasonic dosimeters's response to neutrons, the development of Spectral Correction Factors, determining the response of Panasonic dosimeters in the range of 1 to 1000 rad, and the development of a least squares technique using four independent spectra to obtain some spectral information from an unknown spectrum. The methodology used to characterize Panasonic's dosimeters for accident dosimetry could also be used for any other type of dosimeter.

CHAPTER II

THEORY

2.1. Thermoluminescent Mechanism

The mechanism of thermoluminescence (TL) is based on the release of trapped radiation within the dosimeter. When the dosimeter is heated, the trapped energy is released in the form of light in a process called thermoluminescence. Thus, the light given off is proportional to the amount of energy absorbed. Many materials possess this thermoluminescent property; however, the most common materials used for dosimetry purposes are LiF, $Li_2B_4O_7$, $CaSO_4$, and CaF_2.

This process of thermoluminescence can be understood by considering the valence and conduction bands. The valence band is the highest energy band normally occupied by electrons, while the conduction band, which is normally not occupied by electrons in a TL material, is directly above the valence band. The range of energies between these two bands is known as the band gap. In a pure TL material, electrons cannot possess energies in this range. However, TLDs are not pure materials and contain many impurities either naturally or intentionally. When impurities are added intentionally, the material is said to be "doped" or to contain activators. Common impurities in TLD's are copper, magnesium, titanium, and dysprosium. When impurities exist in a material, electrons can be trapped by impurities contained within the bandgap.

Electron traps and hole traps are the result of impurities. An electron trap is the consequence of an impurity lacking enough electrons so that incomplete covalent bonds, or holes, are formed with the surrounding atoms in the crystal lattice. If an electron from the valence band gains enough energy to be moved into the conduction band, this electron becomes free and can fall into the electron trap. Whereas the electron trap impurity has insufficient electrons to form covalent bonds within the lattice, the hole trap impurity has more than enough unpaired electrons necessary to form covalent bonds. These extra electrons are not as tightly bound to the lattice; thus, the energies of the hole traps lie just above the valence band. In a given TLD material, both hole traps and electron traps coexist as seen by Figure 2.1 (Frame, 1993) and (Horowitz, Volume I, 1984).

Absorption of radiation by a TLD material gives some of the electrons in the valence band enough energy to be moved to the conduction band. Once in the conduction band, electrons are mobile and can fall into the electron traps, and holes in the valence band can migrate until they reach the hole traps. The result is a filled hole trap and a filled electron trap (Figure 2.2). There are two possible modes of recombination, removing electrons and holes from the traps, when a TLD material is heated, and both of these modes of recombination lead to the emission of light. The first mode of recombination involves the electrons in the filled electron traps gaining enough energy (in the form of heat) to be moved back into the conduction band. These electrons can then migrate to a filled hole trap where recombination occurs with the emission of a photon (Figure 2.3). An alternate mode of recombination involves the holes in a filled trap gaining enough energy in the form of heat to migrate to a trapped electron where

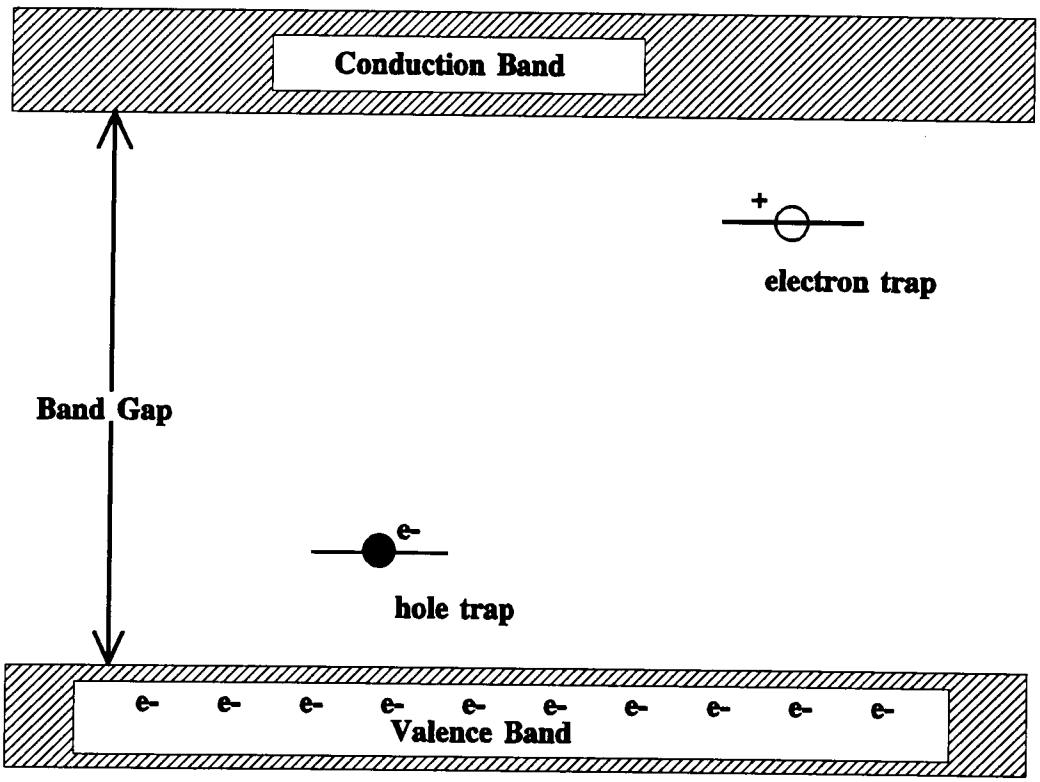


Figure 2.1 Diagram Showing Both Electron and Hole Traps in a TLD Material.

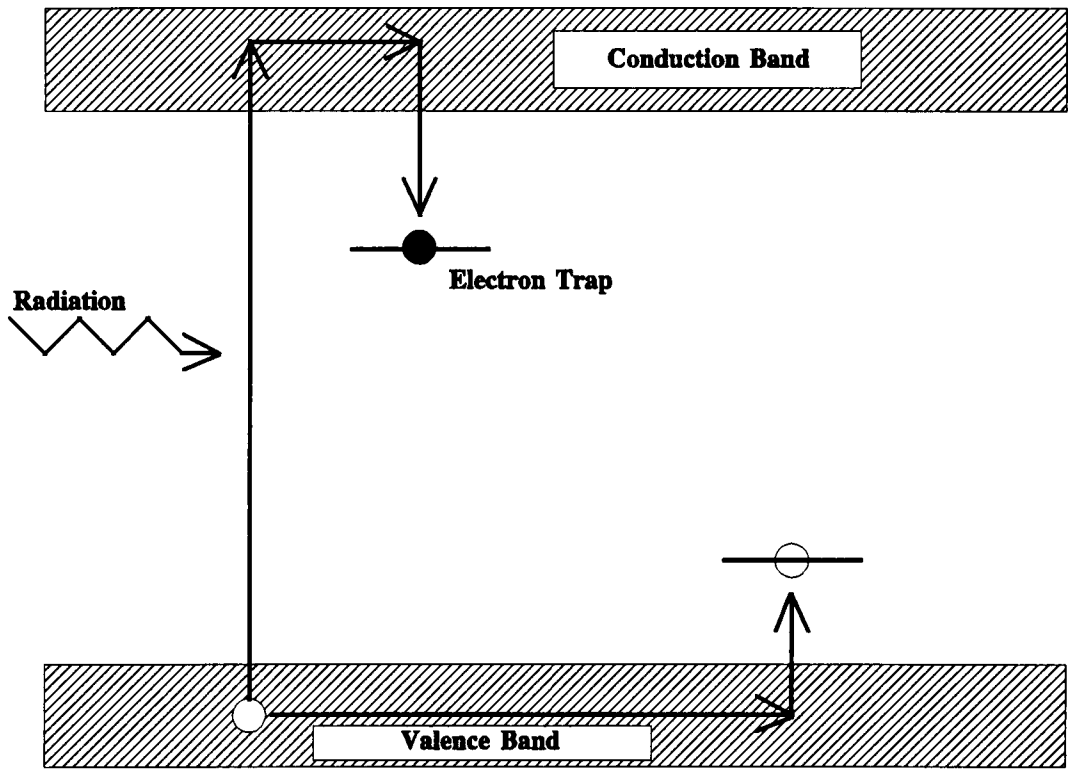


Figure 2.2 Formation of an Electron-Hole Pair in a TLD Material When Exposed to Radiation.

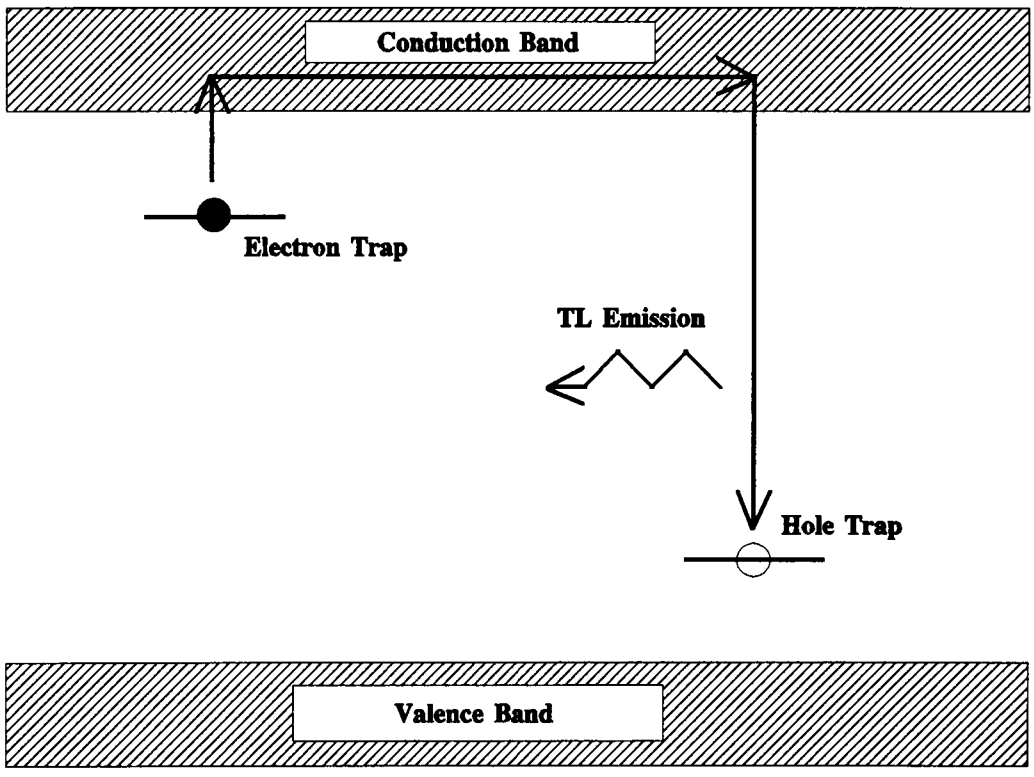


Figure 2.3 First Possible Mode of Recombination When Heat Is Applied.

recombination occurs and a photon is emitted (Figure 2.4). This light emitted by either mode of recombination of trapped electron/holes can thus be measured and can be related back to the energy absorbed by the TLD material (Knoll, 1989).

2.2. Energy Deposition of Lithium Tetraborate

Accident dosimetry involves measuring large doses of both gamma and neutron radiation. For the Panasonic dosimeter UD-809AS to be used as an accident dosimeter, the response of $Li_2B_4O_7$ to neutrons must be known. The determination of the response of $Li_2B_4O_7$ to neutrons is accomplished by calculating the energy deposition in terms of kerma per unit fluence. Kerma stands for Kinetic Energy Released per unit MAss and is the "initial kinetic energy of all charged particles liberated by the radiation per unit mass" (Turner, 1986). This work follows the methodology of Tanaka and Furuta (1972, 1977) in their calculation of the response of ^6LiF to neutrons. The kerma per unit fluence, ($K(E_n)$), for each *i*th reaction is calculated by Equation 2.1.

$$K(E_n)_{i,j} = C\,\varepsilon_{i,j}(E_n + Q_{i,j})\sigma_{i,j}(E_n)D_j \qquad (2.1)$$

where E_n = neutron energy (MeV)

C = conversion factor from MeV to ergs = 1.6021×10^{-6} ergs/MeV

$Q_{i,j}$ = Q value of the *i*th reaction for the *j*th nucleus

$\varepsilon_{i,j}$ = fractional energy transfer of the *i*th reaction for the *j*th nucleus for elastic scattering (set to unity for reactions other than elastic scattering)

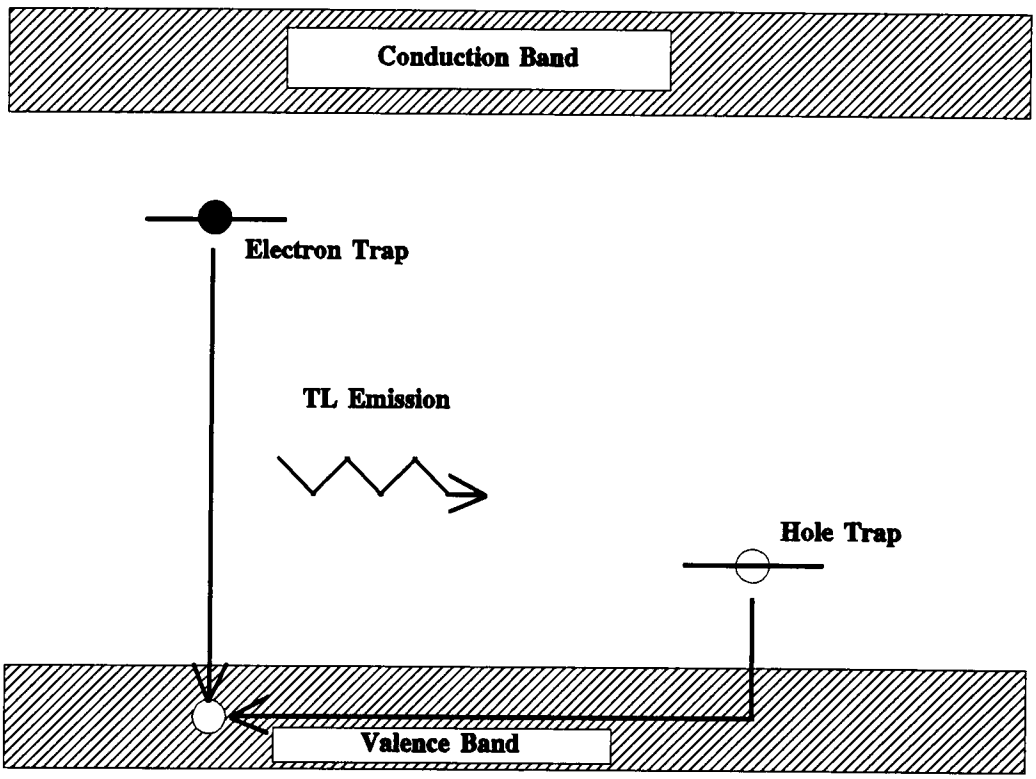


Figure 2.4 Second Possible Mode Recombination When Heat Is Applied.

$\sigma_{i,j}$ = microscopic cross section of the *i*th reaction with the *j*th nucleus (cm^2)

D_j = atomic density for the *j*th nucleus (atoms of ^6Li, ^{10}B, or ^{16}O per gram of $Li_2B_4O_7$)

(Tanaka and Furuta, 1972).

The microscopic cross sections and Q values for all interactions come from the National Nuclear Data Center (NNDC) using the Evaluated Nuclear Data Files (ENDF/B-VI) normalized to 300° K. Energy values used for evaluating this function are chosen to correlate with energy groups in the International Atomic Energy Agency's *Compendium of Neutron Spectra and Detector Responses for Radiation Protection Purposes* (IAEA, 1990). The calculation for the atomic densities for ^6Li, ^{10}B, and ^{16}O are shown below, which assumes that both ^6Li and ^{10}B are enriched between 95-96% (Wasek, 1994) and that natural oxygen is 99.76% ^{16}O (Walker, Parrington, and Feiner, 1989):

$$D_{^6Li} = \left[\frac{1 \text{ mole}}{164.07792 \text{ g } Li_2B_4O_7}\right] \times \left[\frac{6.0223 \times 10^{23} \text{ molecules}}{1 \text{ mole } Li_2B_4O_7}\right] \times \left[\frac{2 \text{ atoms of Li}}{1 \text{ molecule } Li_2B_4O_7}\right] \times \left[\frac{0.95 \text{ atoms } ^6Li}{1 \text{ atoms Li}}\right] = 6.97 \times 10^{21} \frac{\text{atoms } ^6Li}{\text{g } Li_2B_4O_7} \quad (2.2)$$

$$D_{^{10}B} = \left[\frac{1 \text{ mole}}{164.07792 \text{ g } Li_2B_4O_7}\right] \times \left[\frac{6.0223 \times 10^{23} \text{ molecules}}{1 \text{ mole } Li_2B_4O_7}\right] \times \left[\frac{4 \text{ atoms of B}}{1 \text{ molecule } Li_2B_4O_7}\right] \times \left[\frac{0.95 \text{ atoms } ^{10}B}{1 \text{ atom B}}\right] = 1.39 \times 10^{22} \frac{\text{atoms } ^{10}B}{\text{g } Li_2B_4O_7} \quad (2.3)$$

$$D_{^{16}O} = \left[\frac{1 \text{ mole}}{164.07792 \text{ g } Li_2B_4O_7}\right] \times \left[\frac{6.0223 \times 10^{23} \text{ molecules}}{1 \text{ mole } Li_2B_4O_7}\right] \times \left[\frac{7 \text{ atoms of O}}{1 \text{ molecule } Li_2B_4O_7}\right] \times \left[\frac{0.9976 \text{ atoms } ^{16}O}{1 \text{ atom O}}\right] = 2.53 \times 10^{21} \frac{\text{atoms } ^{16}O}{\text{g } Li_2B_4O_7} \quad (2.4)$$

The fractional energy transfer to the recoil nucleus, ε, is used in calculating the energy deposition for elastic scattering. The fractional energy transfer can be found by calculating the average final neutron energy ($\overline{E_f}$) in terms of the initial neutron energy (E_i) by solving equations that describe the two particle kinetics for elastic scattering (Duderstadt and Hamilton, 1976) and (Miller, 1994). The fractional energy transfer is defined in Equation 2.5

$$\varepsilon = \frac{\overline{E_R}}{E_i} = \frac{E_i - \overline{E_f}}{E_i} \quad (2.5)$$

where $\overline{E_R}$ is the average energy of the recoil nucleus. Duderstadt and Hamilton (1976) and Miller (1994) determined the average final neutron energy as found in Equation 2.6.

$$\overline{E_f} = \left[\frac{1 + \alpha}{2}\right] E_i \quad (2.6)$$

where α is defined in Equation 2.7 in terms of A which is the ratio of the mass target to the neutron mass.

$$\alpha = \left[\frac{A - 1}{A + 1}\right]^2 \quad (2.7)$$

The average energy loss or the energy of the recoil nucleus is found by subtracting the

average final energy from the initial energy of the neutron as seen in Equation 2.8.

$$\overline{E_R} = E_i - \overline{E_f} = E_i - \left[\frac{1+\alpha}{2}\right] E_i = \left[\frac{1+\alpha}{2}\right] E_i \tag{2.8}$$

By substituting the average energy of the recoil into Equation 2.5, the fractional energy transfer can be found.

$$\varepsilon = \left[\frac{1-\alpha}{2}\right] \tag{2.9}$$

Thus, by substituting in values of α into Equation 2.9, the fractional energy transfer for given isotopes can be found. Table 2.1 contains values for A, α, and ε for the recoil nuclei of interest: ^{6}Li, ^{10}B, ^{16}O, ^{7}Li, and ^{11}B.

The primary interactions of interest are the $^{10}B(n,\alpha)^{7}Li$ and $^{6}Li(n,\alpha)t$ at lower energies and the elastic scattering of ^{10}B, ^{6}Li, and ^{16}O at higher energies. Table 2.2 contains all interactions along with their Q values used in the calculation of the energy deposited per unit fluence for $^{6}Li_2{}^{10}B_4O_7$. The total kerma per unit fluence is found by summing all *i* interactions for each nucleus as seen by Equation 2.10.

$$K(E_n)_{\text{total}} = \sum_{i,j} K(E_n)_{i,j} \tag{2.10}$$

The energy deposited per unit fluence for $^{6}Li_2{}^{10}B_4O_7$, along with the contribution due to its three components (^{6}Li, ^{10}B, and ^{16}O), is given in Figure 2.5. Using the same methodology, the energy deposition for $^{7}Li_2{}^{11}B_4O_7$ can also be found. The interactions, along with the Q values, are found in Table 2.3. The resulting curves for both $^{6}Li_2{}^{10}B_4O_7$ and $^{7}Li_2{}^{11}B_4O_7$ are found in Figure 2.6 which shows that $^{6}Li_2{}^{10}B_4O_7$ responds very well to

Table 2.1 Values for A, α, and ε for Lithium, Boron, and Oxygen.

ISOTOPE	A	α	ε
^{6}Li	5.96345	0.508064	0.245968
^{10}B	9.92692	0.667433	0.166283
^{16}O	15.8575	0.776793	0.116040
^{7}Li	6.95573	0.560415	0.219792
^{11}B	10.9147	0.692458	0.153771

Table 2.2 Interactions Along with Q Values Used in the Calculation of Kerma Per Unit Fluence for $^{6}Li_{2}{}^{10}B_{4}O_{7}$.

Interaction	Q value (MeV)
$^{6}Li(n,\alpha)t$	4.7838
$^{6}Li(n,\gamma)^{7}Li$	7.2506
$^{6}Li(n,p)^{6}He$	-2.7273
$^{6}Li(n,2n\alpha)p$	-3.6980
$^{6}Li(n,elastic)$	0
$^{10}B(n,\alpha)^{7}Li$	2.790
$^{10}B(n,\gamma)^{11}B$	11.4560
$^{10}B(n,p)^{10}Be$	0.2262
$^{10}B(n,t2\alpha)$	-4.3610
$^{10}B(n,d)^{9}Be$	0.3240
$^{10}B(n,elastic)$	0
$^{16}O(n,\gamma)^{17}O$	4.1434
$^{16}O(n,d)^{15}N$	-9.9030
$^{16}O(n,p)^{16}N$	-9.6368
$^{16}O(n,\alpha)^{13}C$	-2.2156
$^{16}O(n,elastic)$	0

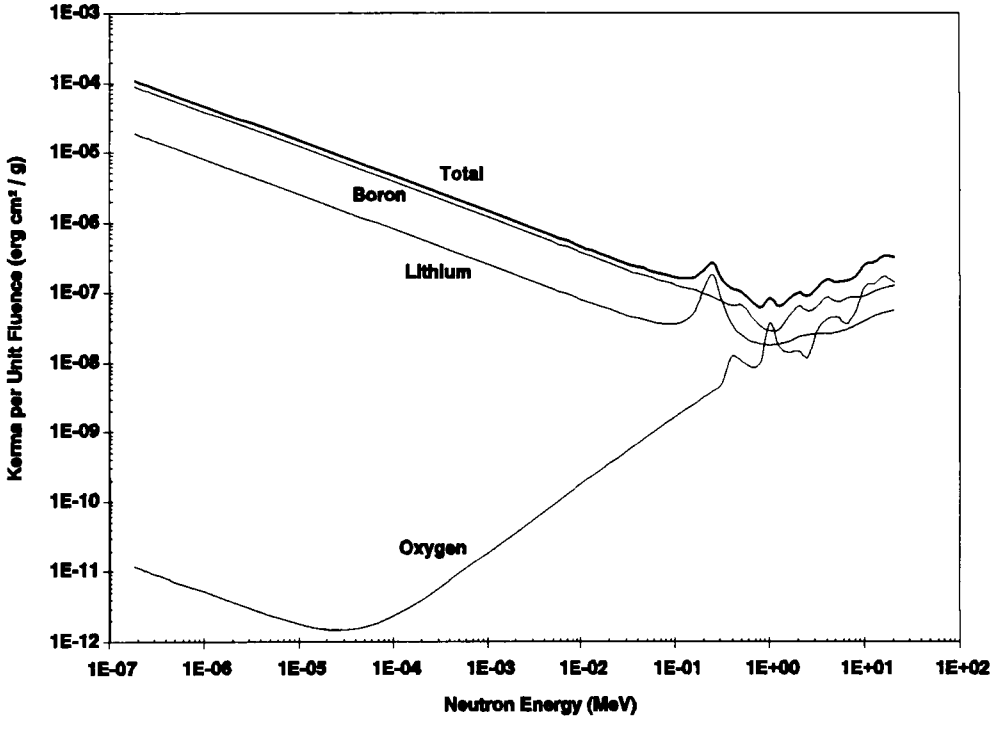


Figure 2.5 Energy Deposition for $^{6}Li_{2}{}^{10}B_{4}O_{7}$ Along with the Contribution for Each Element: ^{6}Li, ^{10}B, and ^{16}O.

Table 2.3 Interactions Along with Q Values Used in the Calculation of Kerma Per Unit Fluence for $^{7}Li_{2}{}^{11}B_{4}O_{7}$.

Interaction	Q value (MeV)
$^{7}Li(n,2n)^{6}Li$	-7.2505
$^{7}Li(n,2n\alpha)^{2}H$	-8.7240
$^{7}Li(n,3n\alpha)^{1}H$	-10.9486
$^{7}Li(n,d)^{6}He$	-7.7532
$^{7}Li(n,\gamma)^{8}Li$	2.0328
$^{7}Li(n,elastic)$	0
$^{11}B(n,2n)^{10}B$	-11.4541
$^{11}B(n,n\alpha)^{7}Li$	-8.6637
$^{11}B(n,np)^{10}Be$	-11.228
$^{11}B(n,p)^{11}Be$	-10.7237
$^{11}B(n,\gamma)^{12}B$	3.3699
$^{11}B(n,t)^{9}Be$	-9.5582
$^{11}B(n,\alpha)^{8}Li$	-6.6309
$^{11}B(n,elastic)$	0
$^{16}O(n,\gamma)^{17}O$	4.1434
$^{16}O(n,d)^{15}N$	-9.9030
$^{16}O(n,p)^{16}N$	-9.6368
$^{16}O(n,\alpha)^{13}C$	-2.2156
$^{16}O(n,elastic)$	0

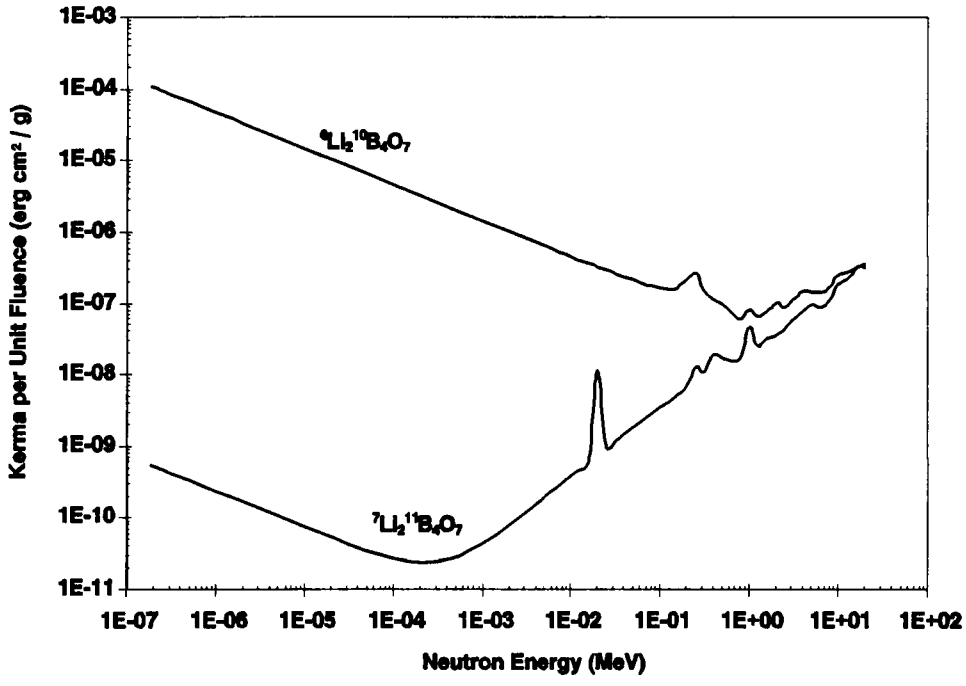


Figure 2.6 Energy Deposition for Both $^{6}Li_2{}^{10}B_4O_7$ and $^{7}Li_2{}^{11}B_4O_7$.

neutrons as compared to $^{7}Li_2{}^{11}B_4O_7$.

2.3. Integral Thermoluminescence

The integral thermoluminescence $G(E_n,\lambda)$ of a TLD in a light wave band (λ) can be determined in the following manner according to Tanaka and Furuta:

$$G(E_n,\lambda)_{Li_2B_4O_7} = a(\lambda)\ g(\lambda)_{LiBO(i)}\ C_{LiBO(i)}\ K(E_n)_{total} \qquad (2.11)$$

where $K(E_n)_{total}$ = kerma per unit fluence for all interactions of $^{6}Li_2{}^{10}B_4O_7$ with neutron energy E_n,

$a(\lambda)$ = self absorption factor of $^{6}Li_2{}^{10}B_4O_7$ for luminescent light in wave band λ,

$g(\lambda)_{LiBO(i)}$ = conversion efficiency from kerma by *i*th reaction to $^{6}Li_2{}^{10}B_4O_7$ integral thermoluminescence in wave band λ, and

$C_{LiBO(i)}$ = correction factor to obtain true imparted energy by the *i*th particle to $^{6}Li_2{}^{10}B_4O_7$ TLD from corresponding kerma value

However, these three factors ($a(\lambda)$, $g(\lambda)$, and C) are not known independently, but an overall conversion efficiency from kerma to integral thermoluminescence ($\eta(\lambda)$ in units of rad ^{137}Cs/erg/g) can be determined where

$$\eta(\lambda) = a(\lambda)\ g(\lambda)\ C \qquad (2.12)$$

(Tanaka and Furuta, 1972 and 1977). The calculation of the overall conversion efficiency factor, ($\eta(\lambda)$), involves the following five step process. Results of each step are found in Table 2.4.

Table 2.4 Overall Conversion Efficiency, $\eta(\lambda)$, from Kerma to Integral Thermoluminescence for Panasonic's UD-809AS.

	Element 2	Element 3	Element 4
Step 1 (erg/g/source n)	4.64×10^{-7}		
Step 2 (mR^*/ ^{137}Cs mrad)	0.756	0.698	0.763
Step 3 (mR^*/source n)	2.86×10^{-6}	2.84×10^{-6}	5.94×10^{-6}
Step 4 (^{137}Cs mrad/source n)	3.78×10^{-6}	4.06×10^{-6}	7.78×10^{-6}
Step 5 $\eta(\lambda)$ (^{137}Cs rad/erg/g)	8.14×10^{-3}	8.75×10^{-3}	1.68×10^{-2}

Step 1

Obtain the dosimeter response to D_2O-moderated ^{252}Cf that considers both the direct radiation from the source and also backscattered radiation off the phantom due to the source. The dosimeter response is found by summing the product of kerma per unit fluence ($K(E_n)$ in units of erg/g / n/cm^2) and the D_2O-moderated modified spectrum ($\Phi(E)$ in units of n/cm^2 /source n) over all energies.

$$\text{Response} = \sum K(E_n)_{\text{total}}\ \Phi(E) \quad \left[\frac{\text{erg/g}}{\text{source n}}\right] \tag{2.13}$$

The normal D_2O-moderated spectrum is modified to include not only the direct radiation but also the effects of the phantom on the spectrum in the form of a scattered spectrum. A scattered spectrum is approximated by using tabulated spectra on the front face of an elliptical phantom for broad parallel beams. The D_2O-moderated ^{252}Cf spectrum and the scattered spectra are from the IAEA Technical Report Number 318 (1990).

Step 2

Expose dosimeters to a known amount of ^{137}Cs. Dosimeters are exposed in holders on a PMMA (polymethyl methacrylate) phantom to 515 mrad. By obtaining light output (in units of mR* for the Panasonic reader) for all elements of four UD-809AS dosimeters, the average response of each element to a known dose of ^{137}Cs is found in units of mR*/mrad ^{137}Cs.

Step 3

Expose dosimeters to a known amount of D_2O-moderated ^{252}Cf to get the average light output (mR*) for each element. Four UD-809AS dosimeters are exposed to 500

mrem of D_2O-moderated ^{252}Cf at 0.5 m which corresponds to 1.955×10^8 source neutrons emitted. Thus, the ratio of light output to source neutrons emitted is calculated in units of mR^*/source neutron for a given neutron spectrum.

Step 4

Divide Step 3 results by Step 2 results to obtain a ratio of cesium dose to D_2O-moderated ^{252}Cf dose as seen from Equation 2.14.

$$\frac{\dfrac{mR^*}{\text{source n}}}{\dfrac{mR^*}{^{137}Cs\ mrad}} = \frac{^{137}Cs\ mrad}{\text{source n}} \tag{2.14}$$

Step 5

The overall conversion efficiency is determined by dividing Step 4 results by Step 1 results.

$$\eta(\lambda) = \frac{^{137}Cs\ mrad}{\text{source n}} \div \frac{\text{erg/g}}{\text{source n}} = \frac{^{137}Cs\ mrad}{\text{erg/g}} \tag{2.15}$$

Thus, after determining the overall conversion factor, the integral thermoluminescence is determined by Equation 2.16.

$$G(E_n, \lambda)_{Li_2B_4O_7} = \eta(\lambda)\ K(E_n)_{total} \tag{2.16}$$

2.4. Response of $Li_2B_4O_7$ to Possible Accident Scenarios

In order to calculate the neutron dose using the Panasonic UD-809AS dosimeter for a criticality accident, the response of the dosimeter to various accident spectra must

be known. Since it is not feasible to test this type of dosimeter with all possible types of accident scenarios, the IAEA's "Compendium of Neutron Spectra in Criticality Accident Dosimetry" is used (IAEA, 1978). An accurate scenario for almost any accident is provided by selecting one of the 115 different shielded and unshielded fission spectra. A complete listing of all 115 spectra types are found in Table 2.5. Each spectrum is in units of n/cm^2 per source neutron in forty-nine energy groups. These energy groups correspond to the groups used in the calculation of the energy deposition of $Li_2B_4O_7$.

In order to compare the UD-809AS's response to possible accident scenarios, the actual dose for each accident scenario from the IAEA must be determined. This is accomplished by applying the appropriate fluence-to-dose conversion factors. The fluence-to-dose conversion factors are obtained from ICRP 21 by log-log interpolation of dose equivalent-to-fluence conversion factors and Quality factors for each given energy (ICRP, 1971). After applying the conversion factors to the accident spectrum, the total actual dose of each scenario is found by integrating these products over all energies (Equation 2.17).

$$\text{Actual Absorbed Dose}_i = \int \frac{\Phi(E_n)_i}{h_\Phi(E_n) Q(E_n) C} dE_n \qquad (2.17)$$

where $\Phi(E_n)_i$ = spectrum for the *i*th accident scenario (n/cm^2/ source n)

$Q(E_n)$ = Quality factor

$h_\Phi(E_n)$ = dose equivalent-to-fluence conversion factor (neutrons/cm^2 sec per mrem/hour)

Table 2.5 Accident Scenarios with Doses, Response of UD-809AS, and SCFs.

Description of Accident Scenario	File Number	Actual Dose (rad/source neutron)	809AS Response (rad/source neutron)	SCF
Uncollided Fission Spectra	1	3.719E-09	5.667E-10	2.805E+02
Fissile Solution, 2 cm radius sphere, H_2O	2	3.390E-09	2.067E-09	7.009E+01
Fissile Solution, 5 cm radius sphere, H_2O	3	2.699E-09	6.971E-09	1.655E+01
Fissile Solution, 10 cm radius sphere, H_2O	4	2.152E-09	8.368E-09	1.099E+01
Fissile Solution, 30 cm radius sphere, H_2O	5	8.375E-10	4.112E-09	8.706E+00
Fissile Solution, 50 cm radius sphere, H_2O	6	5.141E-10	2.668E-09	8.234E+00
Fissile Solution, 2 cm radius sphere, D_2O	7	3.419E-09	6.960E-10	2.100E+02
Fissile Solution, 5 cm radius sphere, D_2O	8	2.945E-09	1.123E-09	1.121E+02
Fissile Solution, 10 cm radius sphere, D_2O	9	2.369E-09	4.871E-09	2.079E+01
Fissile Solution, 30 cm radius sphere, D_2O	10	1.169E-09	6.087E-09	8.208E+00
Fissile Solution, 50 cm radius sphere, D_2O	11	7.761E-10	1.243E-08	2.668E+00
Unshielded HPRR Spectra	12	2.701E-09	1.704E-08	6.775E+00
Concrete-Shielded HPRR Spectra	13	5.502E-10	2.627E-08	8.951E-01
Plexiglass-Shielded HPRR Spectra	14	2.041E-09	1.207E-07	7.224E-01
Steel-Shielded HPRR Spectra	15	1.160E-09	1.078E-08	4.598E+00
Fission Spectra through 2 cm H_2O	16	3.155E-09	2.492E-09	5.411E+01
Fission Spectra through 5 cm H_2O	17	2.016E-09	8.750E-09	9.847E+00
Fission Spectra through 10 cm H_2O	18	2.960E-10	1.492E-09	8.479E+00

Description of Accident Scenario	File Number	Actual Dose (rad/source neutron)	809AS Response (rad/source neutron)	SCF
Fission Spectra through 30 cm H_2O	19	8.609E-11	2.065E-09	1.781E+00
Fission Spectra through 50 cm H_2O	20	7.525E-12	1.676E-11	1.919E+01
Fission Spectra through 2 cm H_2O at Surface	21	3.338E-09	2.520E-09	5.662E+01
Fission Spectra through 2 cm D_2O	22	3.349E-09	7.585E-10	1.887E+02
Fission Spectra through 5 cm D_2O	23	1.765E-09	9.233E-09	8.17E+00
Fission Spectra through 10 cm D_2O	24	7.641E-10	2.822E-08	1.157E+00
Fission Spectra through 30 cm D_2O	25	3.261E-10	2.029E-08	6.869E-01
Fission Spectra through 50 cm D_2O	26	3.171E-11	2.725E-09	4.973E-01
Fission Spectra through 2 cm D_2O At Surface	27	3.563E-09	8.866E-10	1.718E+02
Fission Spectra through 5 cm Graphite	28	2.410E-09	5.667E-10	1.817E+02
Fission Spectra through 10 cm Graphite	29	2.053E-09	4.169E-10	2.105E+02
Fission Spectra through 20 cm Graphite	30	9.232E-10	2.722E-09	1.449E+01
Fission Spectra through 40 cm Graphite	31	2.121E-10	3.581E-08	2.532E-01
Fission Spectra through 60 cm Graphite	32	8.091E-11	5.777E-08	5.986E-02
Fission Spectra through 5 cm CH_2	33	1.262E-09	7.302E-08	7.387E-01
Fission Spectra through 10 cm CH_2	34	4.289E-10	8.534E-08	2.148E-01

Description of Accident Scenario	File Number	Actual Dose (rad/source neutron)	809AS Response (rad/source neutron)	SCF
Fission Spectra through 20 cm CH_2	35	4.883E-11	1.579E-08	1.322E-01
Fission Spectra through 40 cm CH_2	36	7.118E-13	1.921E-10	1.584E-01
Fission Spectra through 60 cm CH_2	37	1.618E-14	3.105E-12	2.227E-01
Fission Spectra through 5 cm of 1% Borated CH_2	38	1.275E-09	8.129E-09	6.704E+00
Fission Spectra through 10 cm of 1% Borated CH_2	39	4.684E-10	3.871E-09	5.172E+00
Fission Spectra through 20 cm of 1% Borated CH_2	40	9.239E-11	3.990E-10	9.896E+00
Fission Spectra through 40 cm of 1% Borated CH_2	41	8.886E-13	5.569E-12	6.820E+00
Fission Spectra through 60 cm of 1% Borated CH_2	42	2.247E-14	1.220E-13	7.869E+00
Fission Spectra through 2.5 cm of 1% Be	43	2.460E-09	4.281E-10	2.456E+02
Fission Spectra through 5 cm Be	44	1.706E-09	4.422E-10	1.649E+02
Fission Spectra through 10 cm Be	45	9.097E-10	5.827E-09	6.673E+00
Fission Spectra through 20 cm Be	46	2.510E-10	5.350E-08	2.005E-01
Fission Spectra through 30 cm Be	47	1.078E-10	8.846E-08	5.208E-02
Fission Spectra through 2.5 cm Al	48	2.974E-09	4.497E-10	2.827E+02

Description of Accident Scenario	File Number	Actual Dose (rad/source neutron)	809AS Response (rad/source neutron)	SCF
Fission Spectra through 5 cm Al	49	2.423E-09	3.785E-10	2.736E+02
Fission Spectra through 10 cm Al	50	1.699E-09	3.043E-10	2.386E+02
Fission Spectra through 20 cm Al	51	9.160E-10	2.701E-10	1.449E+02
Fission Spectra through 30 cm Al	52	3.031E-10	3.430E-10	3.776E+01
Fission Spectra through 10 cm Concrete	53	2.677E-09	4.308E-09	2.656E+01
Fission Spectra through 20 cm Concrete	54	1.729E-09	1.507E-08	4.902E+00
Fission Spectra through 30 cm Concrete	55	7.750E-10	1.385E-08	2.392E+00
Fission Spectra through 40 cm Concrete	56	3.619E-10	7.559E-09	2.046E+00
Fission Spectra through 60 cm Concrete	57	7.335E-11	1.430E-09	2.192E+00
Fission Spectra through 5 cm Concrete with 10% Fe	58	2.073E-09	1.086E-09	8.162E+01
Fission Spectra through 10 cm Concrete with 10% Fe	59	1.248E-09	8.703E-09	6.129E+00
Fission Spectra through 20 cm Concrete with 10% Fe	60	4.798E-10	3.682E-08	5.569E-01
Fission Spectra through 60 cm Concrete with 10% Fe	61	1.387E-11	4.461E-09	1.329E-01
Fission Spectra through 100 cm Concrete with 10% Fe	62	1.446E-13	8.977E-11	6.885E-02

Description of Accident Scenario	File Number	Actual Dose (rad/source neutron)	809AS Response (rad/source neutron)	SCF
Fission Spectra through 5 cm Concrete with 50% Fe	63	2.010E-09	8.287E-10	1.037E+02
Fission Spectra through 10 cm Concrete with 50% Fe	64	1.287E-09	5.187E-09	1.060E+01
Fission Spectra through 20 cm Concrete with 50% Fe	65	4.646E-10	9.726E-08	2.042-01
Fission Spectra through 60 cm Concrete with 50% Fe	66	4.040E-12	6.727E-10	2.567E-01
Fission Spectra through 100 cm Concrete with 50% Fe	67	2.728E-14	5.520E-12	2.112E-01
Fission Spectra through 100 cm Concrete with 100% Fe	68	3.043E-12	1.063E-10	1.224E+00
Fission Spectra through 5 cm Fe	69	3.182E-09	6.035E-10	2.254E+02
Fission Spectra through 10 cm Fe	70	2.626E-09	6.449E-10	1.740E+02
Fission Spectra through 20 cm Fe	71	1.630E-09	7.257E-10	9.599E+01
Fission Spectra through 30 cm Fe	72	9.722E-10	6.778E-10	6.130E+01
Fission Spectra through 50 cm Fe	73	4.522E-10	5.136E-10	3.763E+01
Fission Spectra through 5 cm Cu	74	3.068E-09	6.695E-10	1.959E+02
Fission Spectra through 10 cm Cu	75	2.447E-09	8.086E-10	1.293E+02

Description of Accident Scenario	File Number	Actual Dose (rad/source neutron)	809AS Response (rad/source neutron)	SCF
Fission Spectra through 20 cm Cu	76	1.446E-09	1.150E-09	5.376E+01
Fission Spectra through 30 cm Cu	77	7.422E-10	1.309E-09	2.424E+01
Fission Spectra through 50 cm Cu	78	2.443E-10	9.840E-10	1.061E+01
Fission Spectra through 5 cm Pb	79	3.526E-09	5.827E-10	2.586E+02
Fission Spectra through 10 cm Pb	80	3.311E-09	6.017E-10	2.352E+02
Fission Spectra through 20 cm Pb	81	2.856E-09	6.754E-10	1.807E+02
Fission Spectra through 30 cm Pb	82	2.451E-09	7.842E-10	1.336E+02
Fission Spectra through 50 cm Pb	83	1.777E-09	1.153E-09	6.588E+00
Fission Spectra through 5 cm ^{238}U	84	3.223E-09	7.519E-10	1.832E+02
Fission Spectra through 10 cm ^{238}U	85	2.584E-09	9.265E-10	1.192E+02
Fission Spectra through 20 cm ^{238}U	86	1.601E-09	8.815E-10	7.763E+01
Fission Spectra through 30 cm ^{238}U	87	5.274E-10	5.139E-10	4.386E+01
Fission Spectra through 50 cm ^{238}U	88	5.771E-11	7.810E-11	3.158E+01
Fission Spectra, H_2O-Moderated through 2.5 cm Be	89	1.061E-09	5.560E-08	8.156E-01
Fission Spectra, H_2O-Moderated through 5 cm Be	90	7.545E-10	8.963E-08	3.598E-01

Description of Accident Scenario	File Number	Actual Dose (rad/source neutron)	809AS Response (rad/source neutron)	SCF
Fission Spectra, H_2O-Moderated through 10 cm Be	91	3.874E-10	7.639E-08	2.167E-01
Fission Spectra, H_2O-Moderated through 20 cm Be	92	1.328E-10	8.103E-8	7.005E-02
Fission Spectra, H_2O-Moderated through 2.5 cm Al	93	1.521E-09	1.338E-7	4.857E-01
Fission Spectra, H_2O-Moderated through 5 cm Al	94	1.154E-09	1.145E-07	4.306E-01
Fission Spectra, H_2O-Moderated through 10 cm Al	95	9.147E-10	1.094E-07	3.574E-01
Fission Spectra, H_2O-Moderated through 20 cm Al	96	7.620E-10	5.196E-08	6.267E-01
Fission Spectra, H_2O-Moderated through 10 cm Concrete	97	1.485E-09	2.334E-08	2.719E+00
Fission Spectra, H_2O-Moderated through 20 cm Concrete	98	8.196E-10	1.826E-08	1.919E+00
Fission Spectra, H_2O-Moderated through 30 cm Concrete	99	4.076E-10	1.014E-08	1.717E+00
Fission Spectra, H_2O-Moderated through 40 cm Concrete	100	2.358E-10	4.534E-09	2.223E+00

Description of Accident Scenario	File Number	Actual Dose (rad/source neutron)	809AS Response (rad/source neutron)	SCF
Fission Spectra, H_2O-Moderated through 60 cm Concrete	101	4.180E-11	1.155E-09	1.546E+00
Fission Spectra, H_2O-Moderated through 2 cm Fe	102	2.040E-09	2.396E-08	3.640E+00
Fission Spectra, H_2O-Moderated through 20 cm Fe	104	9.065E-10	4.633E-09	8.362E+00
Fission Spectra, H_2O-Moderated through 50 cm Fe	106	2.548E-10	7.714E-10	1.412E+01
Fission Spectra, H_2O-Moderated through 5 cm Cu	107	1.728E-09	9.137E-09	8.083E+00
Fission Spectra, H_2O-Moderated through 10 cm Cu	108	1.467E-09	1.129E-08	5.554E+00
Fission Spectra, H_2O-Moderated through 20 cm Cu	109	8.018E-10	4.312E-9	7.947E+00
Fission Spectra, H_2O-Moderated through 30 cm Cu	110	4.051E-10	1.879E-09	9.213E+00
Fission Spectra, H_2O-Moderated through 50 cm Cu	111	7.472E-11	5.649E-10	5.653E+00
Fission Spectra, H_2O-Moderated through 5 cm Pb	112	2.023E-09	2.459E-08	3.517E+00

Description of Accident Scenario	File Number	Actual Dose (rad/source neutron)	809AS Response (rad/source neutron)	SCF
Fission Spectra, H_2O-Moderated through 10 cm Pb	113	2.136E-09	2.426E-08	3.764E+00
Fission Spectra, H_2O-Moderated through 30 cm Pb	114	1.458E-09	2.092E-08	2.979E+00
Fission Spectra, H_2O-Moderated through 50 cm Pb	115	1.067E-09	1.678E-08	2.718E+00
Bare ^{252}Cf Spectra	116	3.805E-09	6.107E-10	2.663E+02
D_2O-Moderated ^{252}Cf Spectra	117	1.218E-09	5.206E-08	1.000E+01

C = conversion factors [(3600 sec/hour)(1000 mrem/rem)]

The response of the dosimeter to the neutron dose associated with each accident scenario is found by subtracting Element 1 ($^{7}Li_2{}^{11}B_4O_7$) dose from Element 3 ($^{6}Li_2{}^{10}B_4O_7$) dose. Because both of these elements have approximately the same response to gamma radiation and only Element 3 responds to neutrons, the gamma dose can be subtracted from the neutron plus gamma dose.

$$\text{Response to Accident}_{(i)} = \text{Response}_{\text{Element 3}} - \text{Response}_{\text{Element 1}} \tag{2.18}$$

Each of these doses is found by integrating over all energies the product of the integral thermoluminescence ($G(E_n)$ in units of rad / n/cm^2) and the accident spectra ($\Phi(E_n)$ in units of n/cm^2 / source n).

$$\text{Response}_{\text{Element 1 or 3}} = \int G(E_n)\Phi(E_n)\,dE_n \tag{2.19}$$

The accident spectra used for these calculations are the spectra of the direct radiation only and do not include radiation backscattered due to a phantom or the human body. In order to obtain practical SCFs, the effects of the phantom must be accounted for by performing Monte Carlo runs for each of the 115 spectra.

By plotting the actual dose versus the dosimeter response (Figure 2.7), it can be seen that there is no definite relationship between the two for the 115 accident spectra. This lack of relationship implies that the UD-809AS's response is dependent on the type of spectrum. Therefore, a correction factor known as the Spectral Correction Factor (SCF) must be used in order for each different spectrum. The SCF for each spectrum is

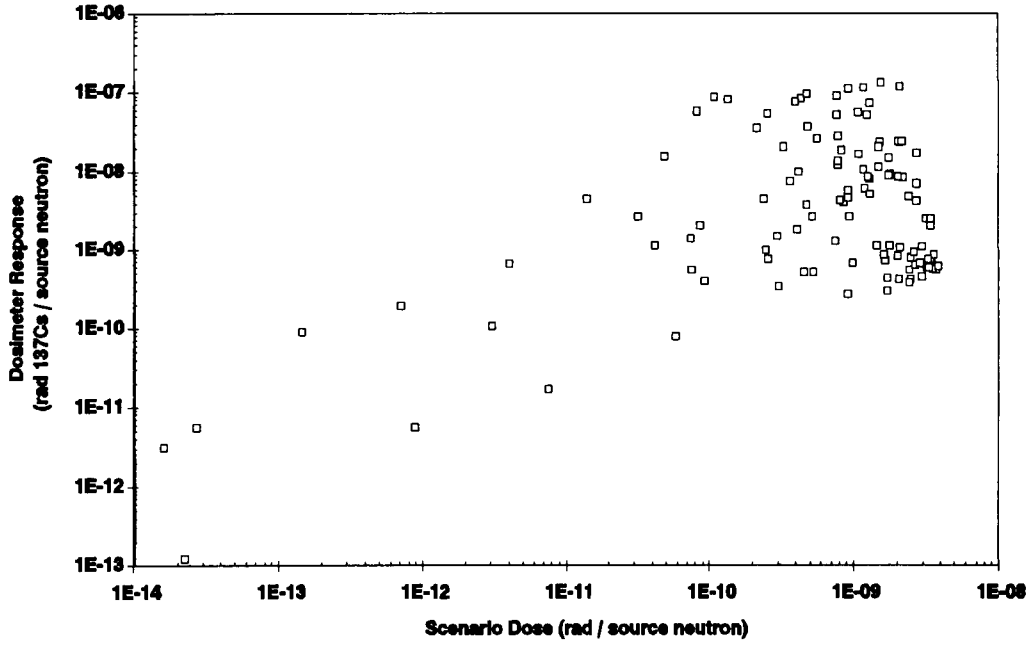


Figure 2.7 Actual Dose Versus the 809AS Response for Each Accident Scenario.

calculated by using Equation 2.20 which normalizes all SCF to D_2O-moderated ^{252}Cf.

$$SCF_i = \frac{D_i R_{D_2O}}{D_{D_2O} R_i} \tag{2.20}$$

where D_i = actual dose of *i*th accident spectrum

R_i = response of the UD-809AS to the *i*th accident spectrum

D_{D2O} = actual dose to D_2O-moderated ^{252}Cf spectrum

R_{D2O} = response of the UD-809AS to D_2O-moderated ^{252}Cf spectrum

(Casson, Mei, and Buckner, 1993).

The actual dose, response of the UD-809AS dosimeter, and Spectral Correction Factors for each *i*th accident scenario are found in Table 2.5. Once SCF's are found for the 115 different spectra, they can be applied to the element response according to Equation 2.21 to obtain the neutron dose in units of rad.

$$D = ((E_3)/(ECF_3) - (E_1)/(ECF_1)) \times C_{D_2O} \times SCF \tag{2.21}$$

where E_1 = Response of Element 1 ($^7Li_2{}^{11}B_4O_7$ - gamma dose)

E_3 = Response of Element 1 ($^6Li_2{}^{10}B_4O_7$ - neutron plus gamma dose)

ECF = Element Correction Factor

C_{D2O} = Conversion Factor for D_2O-moderated Cf (units of rad/mR*)

SCF = Spectral Correction Factor

2.5. Element Correction Factor

The Element Correction Factor (ECF) of a given element is a correction factor that enables all Panasonic dosimeters' elements to respond in a similar manner. ECFs are needed because the TLDs are powder phosphors. The ECFs correct for differences in the amount of phosphor, for uniformity of the phosphor, and for changes in the TLDs with time by comparing the response of each element for every dosimeter to a reference group of elements. ECFs found in this manner are divisors. A corrected response for each element is found by dividing the element response by its ECF. The reference elements are from an arbitrarily chosen set of dosimeters known as the reference set which are used solely for calculating ECFs for the control and field or non-reference dosimeters. The reference set of dosimeters is relatively small compared to the field set and is stored away from other dosimeters to ascertain accidental use. The primary purpose of the control dosimeters is for the calibration of the TLD reader, but the field set is used for personnel monitoring or, in the case of this thesis, for research. The procedure for determining the ECFs is standard for all Panasonic users and is accomplished by the following ten step process (as paraphrased from the Panasonic Industrial Company User's Manual):

2.5.1. Step 1: Irradiate Reference Dosimeters

A reference group, chosen at random from all dosimeters, is irradiated by a radiation source. A recommended source is cesium-137 because its radiation produces a good statistical response in all elements. The dosimeter can be exposed either in air or on a phantom by either a beam irradiator or a panoramic irradiator. In all exposures for the ECF calculations for this research, all dosimeters are exposed in air with the Cesium-

137 panoramic irradiator. The reference group consists of twenty-seven dosimeters (both 802AS and 809AS) and were exposed to 500 mR at 50.9 cm. As with any exposure using $Li_2B_4O_7$, dosimeters' responses are found in units of mR^* after allowing 24 hours after irradiation (to allow initial fading to occur).

2.5.2. Step 2: Calculate Reference Means for Reference Group

The average element response along with standard deviations and coefficient of variation (%CV) are calculated for each element (1-4) for the reference dosimeters. The coefficient of variation is calculated in the following manner:

$$\%CV = \frac{100 \times \text{Standard Deviation}}{\text{Mean}} \tag{2.22}$$

2.5.3. Step 3: Produce ECFs Based on Element Means

Reference group ECFs for each element of every dosimeter is calculated in the following manner:

$$ECF(i,j) = \frac{e(i,j)}{EM(i)} \tag{2.23}$$

where ECF(i,j) = Element Correction Factor for element i of dosimeter j,

e(i,j) = response of element i of dosimeter j, and

EM(i) = mean response of all elements i for all reference dosimeters.

2.5.4. Step 4: Repeat Steps 1 through 3

Steps 1 through 3 are repeated twice to obtain additional ECFs for the reference group. By repeating these steps, statistical variations are reduced. A total of three ECFs for each element of every reference dosimeter is found for better statistics.

2.5.5. Step 5: Average the ECFs for Each Element

The mean ECF for reference dosimeters, along with standard deviations and coefficient of variation, for each element of every dosimeter is calculated for the three irradiations. The results are found in Table 2.6.

2.5.6. Step 6: Examine ECFs and %CVs of Reference Group

At this point, the reference dosimeters' means are examined to ensure that none are unusually large or small. Likewise, the %CVs also need to be examined for unusually large values. If any dosimeter looks questionable for having either too large or small means or either too large %CV, it may need to be dropped from the reference set. The range of means for the reference set varies from 0.52 to 1.32, and the highest %CV is 8.6%.

2.5.7. Step 7: Irradiate Non-reference Dosimeters

A subset of the reference dosimeters is irradiated along with the field and control dosimeters. Once again, the cesium-137 panoramic irradiator is used to expose the dosimeters in air to 500 mR at 50.9 cm. The element responses for each dosimeter are found after allowing 24 hours post irradiation for initial fading to occur.

2.5.8. Step 8: Calculate Element Means of Reference Set

Because ECFs are already in existence for the reference dosimeters, the corrected response obtained by applying ECFs of the reference dosimeter subset must be used. As stated earlier, the element responses of then subset of reference dosimeters are divided by the ECFs to obtain the corrected response. After ECFs are applied, the mean for each of the four element responses in the reference dosimeter subset are found.

Table 2.6 Reference Group Average ECFs and Standard Deviations.

ID number	ECF1	ECF2	ECF3	ECF4
2	0.624 ± 0.012	0.763 ± 0.009	0.783 ± 0.057	0.677 ± 0.039
6	0.560 ± 0.008	0.856 ± 0.022	0.811 ± 0.036	0.799 ± 0.047
8	0.608 ± 0.013	0.766 ± 0.005	0.751 ± 0.059	0.746 ± 0.062
27	0.626 ± 0.017	0.928 ± 0.016	0.935 ± 0.046	0.920 ± 0.069
45	0.524 ± 0.015	0.706 ± 0.016	0.725 ± 0.036	0.727 ± 0.063
58	0.553 ± 0.006	0.708 ± 0.008	0.817 ± 0.054	0.723 ± 0.045
61	0.559 ± 0.014	0.628 ± 0.023	0.817 ± 0.049	0.607 ± 0.014
618	1.227 ± 0.041	1.029 ± 0.014	0.836 ± 0.042	0.948 ± 0.063
715	1.069 ± 0.011	1.074 ± 0.011	1.043 ± 0.061	1.131 ± 0.060
758	1.223 ± 0.005	1.077 ± 0.004	0.859 ± 0.049	0.987 ± 0.048
828	1.078 ± 0.006	1.024 ± 0.009	0.975 ± 0.037	1.146 ± 0.071
857	1.167 ± 0.027	1.111 ± 0.012	1.051 ± 0.065	1.109 ± 0.053
858	1.221 ± 0.031	1.049 ± 0.019	0.979 ± 0.054	1.091 ± 0.059
918	1.080 ± 0.017	1.062 ± 0.022	0.946 ± 0.050	1.039 ± 0.060
993	1.028 ± 0.008	1.038 ± 0.022	1.069 ± 0.052	1.200 ± 0.069
996	1.150 ± 0.018	1.057 ± 0.045	1.029 ± 0.047	1.150 ± 0.069

ID number	ECF1	ECF2	ECF3	ECF4
1068	1.275 ± 0.033	1.177 ± 0.011	1.122 ± 0.067	1.158 ± 0.066
1092	1.032 ± 0.002	1.064 ± 0.023	0.961 ± 0.052	1.185 ± 0.077
1214	1.189 ± 0.021	1.155 ± 0.026	1.111 ± 0.058	1.198 ± 0.067
1225	1.095 ± 0.032	1.048 ± 0.029	1.071 ± 0.049	1.204 ± 0.077
1258	1.092 ± 0.009	1.062 ± 0.009	1.040 ± 0.071	1.119 ± 0.067
1291	1.231 ± 0.028	1.148 ± 0.021	1.124 ± 0.071	1.204 ± 0.066
1306	1.213 ± 0.014	1.118 ± 0.022	1.017 ± 0.058	1.102 ± 0.053
1374	1.310 ± 0.028	1.141 ± 0.002	1.148 ± 0.069	1.315 ± 0.070
1392	1.099 ± 0.032	1.123 ± 0.18	1.078 ± 0.062	1.165 ± 0.074
1448	1.028 ± 0.028	0.972 ± 0.013	0.968 ± 0.050	1.084 ± 0.056
1460	1.138 ± 0.027	1.116 ± 0.004	1.101 ± 0.071	1.185 ± 0.075

2.5.9. Step 9: Produce ECFs for Non-reference Dosimeters

Element Correction Factors for non-reference dosimeters are calculated by dividing the element response by the element means of the subset of reference dosimeters (with ECFs applied) as seen in Equation 2.24.

$$ECF(i,j) = \frac{e(i,j)}{EM(i)} \tag{2.24}$$

where ECF(i,j) = element correction factor for element i of dosimeter j

e(i,j) = response of element i of dosimeter j

EM(i) = the mean response of all reference dosimeters in the subset for element i

This process allows for the calculation of an ECF for each element of every dosimeter for the non-reference group. Steps 7 through 9 can be repeated for better statistics; however, because of the number of dosimeters to be irradiated, ECFs for the non-reference group are based only upon one irradiation. The justification in only using one irradiation is that a subset of the non-reference dosimeters were tested for variation for the ECFs. The average %CV for the subset is 5.03, 5.59, 3.68, and 3.06 for elements one through four.

2.5.10. Step 10: Examine ECFs of Non-reference Dosimeters

After the ECF calculation is complete, ECFs of the non-reference group need to be examined. From this examination, one may determine if the ECF values are unusually high or low. The range of ECFs in this research vary from 0.367 to 1.248. Now that this process is complete, ECFs are applied to any TLD reading by dividing the element response, (e(i,j)), by the respective ECF to get the true response.

$$\text{True Response}(i,j) = \frac{e(i,j)}{ECF(i,j)} \qquad (2.25)$$

(Panasonic Industrial Company, 1989)

2.6. Supralinearity

At relatively low doses, the response of TLD's are linear with increasing dose; however, at large doses the response is nonlinear with increasing dose. This nonlinear effect of TLD's response to increasing dose is known as supralinearity (Piesch, Burgkhardt, and Kabadjova, 1975). Although many theories exist, the exact cause of supralinearity is unknown. Early theories for supralinearity are based on competition during excitation of the sample (Chen and Fogel, 1993) and competition among the defects or competing traps in the radiative absorption stage (Mische and McKeever, 1989). Both of these authors agree that supralinearity is not caused from these earlier theories, but is characteristic of competition during heating of TLD materials. Further work that supports competition during heating is McKeever (1990) and Horowitz's Track Interaction Model (1990). It is important to note that supralinearity does indeed occur, although the exact cause of supralinearity is unclear at this time.

The extent of supralinearity depends on many factors such as: dose, nature of host material, radiation type (McKeever, 1990), maximum heating temperature during evaluation, pre-exposure annealing process, pre-exposure of the dosimeter, teflon matrix (Piesch,Burgkhardt, and Kabadjova, 1975), temperature of the TL peak, heating rate during TL readout, activators present, and amount of activators in material (Mische and

McKeever, 1989). Although supralinearity measurements have previously been tested for $CaSO_4$ (Burgkhardt, Singh, and Piesch, 1977) and $Li_2B_4O_7$ (Burgkhardt, Piesch, and Singh, 1978), which are the primary elements in Panasonic's dosimeters, these measurements are not applicable to this work because of differences in impurities, in the manufacturing of the elements, and in the actual reading process. Because of these differences, the Panasonic UD-809AS and UD-802AS must be tested for linearity as found in Chapter 4.

2.7 Response Function Using Four Neutron Spectra

With neutron dosimetry, it is helpful to have some spectral knowledge. By knowing the neutron energies, a more accurate dose equivalent can be determined because of the dependence between neutron energy and Quality factor (ICRP 21, 1971). However, getting neutron spectral information from thermoluminescent dosimeters is difficult. Albedo TLDs often contain cadmium and non-cadmium covered elements. The cadmium covered element does not allow thermal neutrons to penetrate because of cadmium's energy cutoff of 0.414 eV. Thus, by using a dosimeter of this nature, the thermal component (non-cadmium covered) can be subtracted from the cadmium covered to obtain a thermal neutron dose. However, this does not give much useful spectral information.

The idea of using the Panasonic UD-809AS's response to four independent neutron spectra in a linear combination has been proposed to obtain more spectral information (Miller, 1993). The four independent spectra being used are bare ^{252}Cf, D_2O-moderated ^{252}Cf, polyethylene-moderated ^{252}Cf, and ^{241}Am-Be. These spectra were chosen because

of their independence and differences among their spectra. Bare ^{252}CF and ^{241}Am-Be have much harder spectra than either D_2O-moderated ^{252}Cf or polyethylene-moderated ^{252}Cf, and only polyethylene-moderated ^{252}Cf has a significant thermal component (IAEA 318, 1990) and (Tanner, et al., 1994). The energy dependent information to be obtained is divided into three energy bins: thermal, epithermal, and fast. The energy of each bin is given in Table 2.7. A linear combination of four different neutron spectra in three energy groups is found in Equation 2.26-28.

$$\Phi^k_{\text{thermal}} = \sum_{i,k=1}^{4} \alpha_{i,\text{thermal}} X_i^k \tag{2.26}$$

$$\Phi^k_{\text{epithermal}} = \sum_{i,k=1}^{4} \alpha_{i,\text{epithermal}} X_i^k \tag{2.27}$$

$$\Phi^k_{\text{fast}} = \sum_{i,k=1}^{4} \alpha_{i,\text{fast}} X_i^k \tag{2.28}$$

where Φ^k_{thermal} = fluence for the *k*th spectrum in each energy group

X^k_i = response of the *i*th element to *k*th spectrum

α_i = coefficient to be determined for each element for each energy group

k = independent spectrum (^{241}Am-Be, bare ^{252}Cf, D_2O-moderated ^{252}Cf, or polyethylene-moderated ^{252}Cf)

i = element number (one through four)

A more useful way of considering this linear combination is in matrix form. The

Table 2.7 Energy Groups and Ranges for Response Function Using Four Neutron Spectra.

Energy Group	Energy Range
thermal	$E_n < 0.414$ eV
epithermal	0.414 eV $< E_n <$ 200 keV
fast	200 keV $< E_n$

following matrix is for thermal energy bins, but matrices for epithermal and fast energy bins are done in a similar fashion.

$$\begin{bmatrix} X_1^{Bare} & X_2^{Bare} & X_3^{Bare} & X_4^{Bare} \\ X_1^{D_2O} & X_2^{D_2O} & X_3^{D_2O} & X_4^{D_2O} \\ X_1^{Am-Be} & X_2^{Am-Be} & X_3^{Am-Be} & X_1^{Am-Be} \\ X_1^{Poly} & X_2^{Poly} & X_3^{Poly} & X_4^{Poly} \end{bmatrix} \begin{bmatrix} \alpha_{1,th} \\ \alpha_{2,th} \\ \alpha_{3,th} \\ \alpha_{4,th} \end{bmatrix} = \begin{bmatrix} \Phi_{th}^{bare} \\ \Phi_{th}^{D_2O} \\ \Phi_{th}^{Am-Be} \\ \Phi_{th}^{Poly} \end{bmatrix} \tag{2.29}$$

The coefficients, α's, can be determined if the element responses and group fluences are known. This is accomplished by first taking the inverse of the square 4 x 4 matrix. This inverse matrix is then multiplied across both sides of Equation 4.4.

$$\begin{bmatrix} X_1^{Bare} & X_2^{Bare} & X_3^{Bare} & X_4^{Bare} \\ X_1^{D_2O} & X_2^{D_2O} & X_3^{D_2O} & X_4^{D_2O} \\ X_1^{Am-Be} & X_2^{Am-Be} & X_3^{Am-Be} & X_1^{Am-Be} \\ X_1^{Poly} & X_2^{Poly} & X_3^{Poly} & X_4^{Poly} \end{bmatrix}^{-1} \begin{bmatrix} \Phi_{th}^{bare} \\ \Phi_{th}^{D_2O} \\ \Phi_{th}^{Am-Be} \\ \Phi_{th}^{Poly} \end{bmatrix} = \begin{bmatrix} \alpha_{1,th} \\ \alpha_{2,th} \\ \alpha_{3,th} \\ \alpha_{4,th} \end{bmatrix} \tag{2.30}$$

These coefficients should be able to determine the fluence for any unknown spectrum and are applied by multiplying the given coefficient by the response of each element in the Panasonic UD-809AS dosimeter.

CHAPTER III

EQUIPMENT AND MATERIALS

3.1. RADCAL

The Dosimetry Applications Research Group (DOSAR) of Oak Ridge National Laboratory's Health Science Research Division operates the Radiation Calibration Laboratory facility (RADCAL). The primary purpose of RADCAL is to "provide facilities for dosimeter intercomparison studies and to perform standard tests for personnel radiation dosimeters to ensure compliance with national accreditation program requirements [National Voluntary Laboratory Accreditation Program (NAVLAP) and Department of Energy Laboratory Accreditation Program (DOELAP)]" while maintaining National Institute of Standards and Technology (NIST) requirements as a secondary calibration laboratory. RADCAL is used by both private industry and ORNL for low level radiobiological experiments, personnel dosimeter research, and radiation instrument calibration.

RADCAL consists of a control room and three irradiation rooms (gamma, X-ray/beta, and neutron) all of which are environmentally monitored and controlled for humidity, temperature, and pressure. The gamma irradiation room (6.4 x 7.0 x 4.3 m) contains both an Amersham beam irradiator and a J. L. Shepherd panoramic irradiator. An EG&G Astro Physic Pantak HF320 X-ray machine and a beta particle irradiator is

stored in the X-ray/beta room (6.4 x 7.0 x 4.3 m). Vendors' addresses and numbers are found in Appendix B. The neutron room (9.1 x 9.1 x 5.8 m) contains two neutron sources stored in the center of the room in a 1.2 m water pool. All sources, with the exception of Pu-Be and Am-Be, are remotely operated and controlled the from control room (6.1 x 2.4 x 4.3 m). (DOSAR Report No. 1-91).

3.2. Sources

The radiological sources used on this project have been calibrated and certified by the National Institute of Standards and Technology (NIST), formerly the National Bureau of Standards, as secondary sources or by NIST traceable instruments. These radiological sources include the following: Amersham beam irradiator, panoramic irradiator, and five neutron sources (^{241}Am-Be, ^{238}Pu-Be, bare ^{252}Cf, D_2O-moderated ^{252}Cf, and polyethylene-moderated ^{252}Cf).

3.2.1. Amersham Beam Irradiator

The Amersham model HBC.5 beam irradiator was calibrated on January 30, 1986 by the Department of Medical Physics, University of Wisconsin, Madison by using a calibrated ion chamber from the National Bureau of Standards (NBS). This calibration is maintained by regular calibration checks using a reference ion chamber calibrated by NIST. The beam irradiator is a 3.7 x 10^{11} Bq (10 Ci) cesium-137 source (half-life = 30.17 years) that has a horizontal beam line with a 20° circular collimator. The center of the beam is approximately 185.5 cm off the floor. The beam irradiator is used to calibrate the Panasonic reader.

3.2.2. J. L. SHEPHERD Panoramic Irradiator

The panoramic irradiator is a 4.4 x 10^{10} Bq (1.2 Ci) cesium-137 source calibrated on December 9, 1981 by J. L. Shepherd and Associates with a NBS traceable meter. the calibration is checked on a routine basis using NIST calibrated ion chambers. The model 142-10 emits an intense beam of gamma radiation through 360° when the source is activated. The ^{137}Cs is operated by a cable type pneumatic cylinder controlled by a solenoid valve. The panoramic irradiator is mounted on a circular table containing a lip at a distance of 50.9 cm from the source. The lip is used to expose as many as one hundred thermoluminescent dosimeters or fifty film badges. The panoramic irradiator is used to calculate the Element Correction Factors (ECFs).

3.2.3. Neutron Sources

The following neutron sources have been used in this research: bare ^{252}Californium, D_2O-moderated ^{252}Californium, polyethylene-moderated ^{252}Californium, ^{241}Americium-Beryllium, and ^{238}Plutonium-Beryllium. Table 3.1 contains the calibration information on these sources. The Cf sources are automatically controlled and operated, but the Am-Be source is manually operated and Pu-Be is operated by a manual remote. The ^{252}Cf configurations involve using a 15 cm D_2O sphere made of stainless steel surrounded by cadmium and a 15 cm polyethylene sphere. For operation, the source is pulled into the center of each sphere. The D_2O-moderated Cf source is used in the supralinearity measurements. The three configurations of ^{252}Cf and ^{241}Am-Be are employed in the linear

Table 3.1 Calibration Information on Neutron Sources.

Source	Half-life (years)	Calibration Emission Rate (n/s)	Calibration Date	Fluence to Dose Conversion Factor (rem cm^2)
Bare ^{252}Cf	2.638	2.51×10^9	05-06-87	3.4×10^{-8} (ISO 8529)
D_2O-moderated ^{252}Cf	2.638	7.63×10^9	04-30-87	9.08×10^{-9} (Eisenhauer, 1984)
Polyethylene-moderated ^{252}Cf	2.638	2.51×10^9	05-06-87	
^{238}Pu-Be	87.7	2.4×10^7	03-22-82	3.76×10^{-8} (Buckner and Sims, 1992)
^{241}Am-Be	432.7	1.271×10^7	05-02-66	3.8×10^{-8} (ANSI N13.11)

combination measurements, and ^{238}Pu-Be is used for verification in the linear combination measurements.

3.3. Panasonic UD-702E Reader

The thermoluminescent dosimeters (TLD) are read one element at a time by the UD-702E manual reader which uses optical heating to release energy stored in the traps of the thermoluminescent (TL) material. The 702E reader uses a tungsten lamp that is filtered by a silicon filter so that the infrared radiation heats the TL phosphor. After the phosphor is heated, energy is released in the form of photons. These photons of light pass through a blue filter which eliminates long wavelengths (red and infrared) of light produced by the heat phosphor, and the photons are then counted by a photomultiplier tube (PMT). A diagram of the optical heating system is found in Figure 3.1. For the reading of each individual phosphor there are three flashes from the tungsten lamp: the pre-heat flash, the TL reading flash, and the post-annealing flash.

A hybrid integrator, which contains both a photon and frequency counter, is used to digitally integrate the output signals from the PMT. The photon counter is used at low exposures while the frequency counter is reserved for high exposures. Each counter is used in the exposure region for which it is linear. The pulse counts from either counter are transferred to a microprocessor which in turn is converted into the Panasonic display in units of mR* (Panasonic Industrial Company, 1989). The Panasonic UD-702E reader is located at ORNL and is maintained by Dosimetry Applications Research (DOSAR). The UD-702E reader was used in every aspect of this research except for the

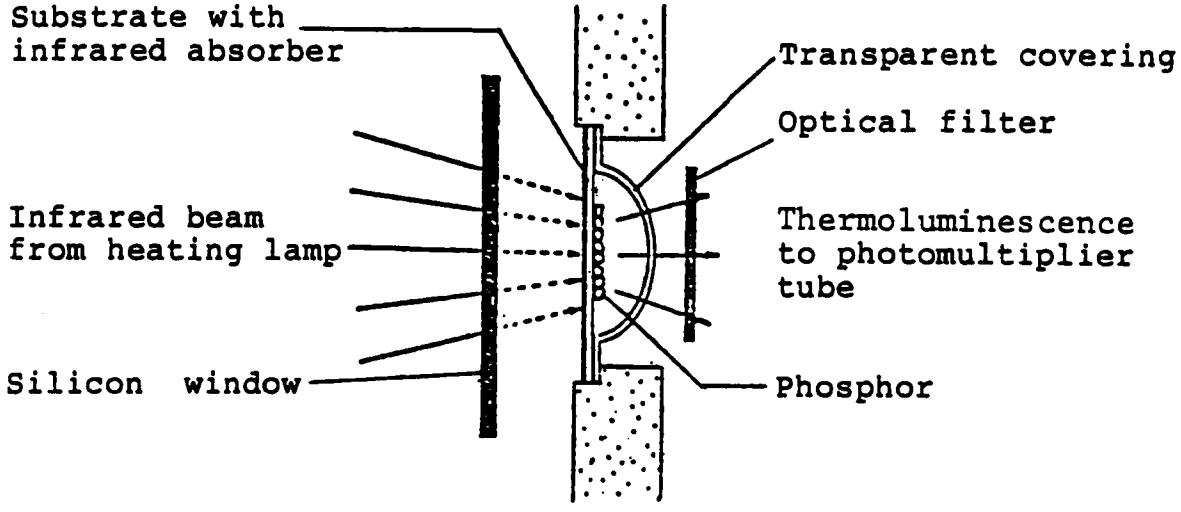


Figure 3.1 Optical Heating Method for the Panasonic UD-809AS (Panasonic Industrial Company, 1989).

supralinearity measurements in the range of 400 to 1000 rad.

3.4. Panasonic UD-710E Reader

The Panasonic UD-710E automatic reader, located at the Tennessee Valley Authority's (TVA) Watts Bar facility, uses the same optical heating method as described in Section 3.3 (Panasonic Industrial Company, 1989). The UD-710E reader was used solely for the supralinearity measurements in the range from 400 to 1000 rad because of the limited electronic capabilities of the older manual 702E reader.

3.5. Panasonic UD-809AS

The Panasonic UD-809AS is a personnel thermoluminescent dosimeter used for measuring neutrons. A diagram of the UD-809AS is found in Figure 3.2. This dosimeter has four chips or elements made of lithium tetraborate activated by copper ($Li_2B_4O_7$:Cu). The four elements are one chip of $^{7}Li_2{}^{11}B_4O_7$ and three chips of $^{6}Li_2{}^{10}B_4O_7$ with front filters consisting of 0.7 mm of cadmium, tin, cadmium, and cadmium, respectively and the back filters consisting of 0.7 mm of cadmium, cadmium, cadmium, and tin, respectively.

Lithium and boron, particularly the isotopes of ^{6}Li and ^{10}B, are commonly used for detection of slow neutrons due to their large capture cross sections, but ^{7}Li and ^{11}B are basically unresponsive to neutrons as seen from Table 3.2. The phosphor

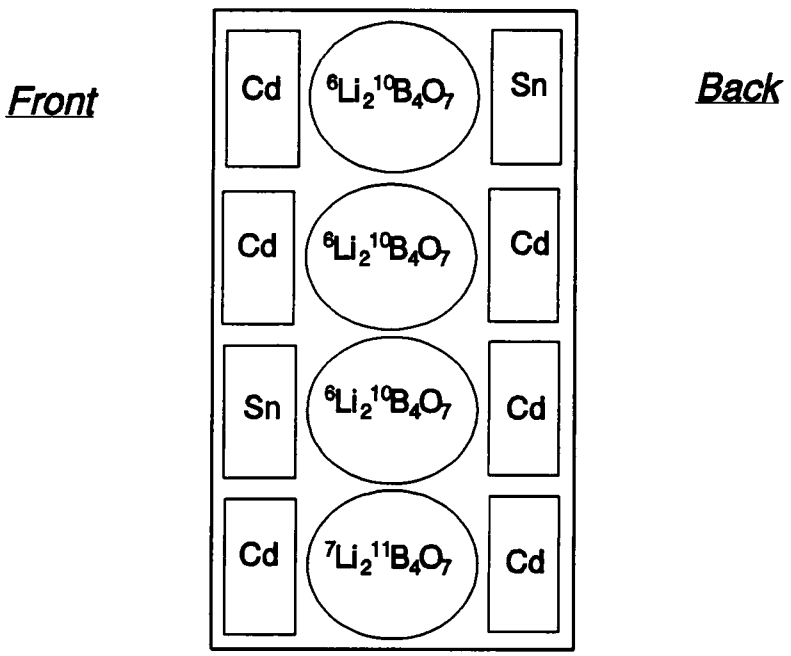


Figure 3.2 Panasonic UD-809AS Thermoluminescent Dosimeter.

Table 3.2 Thermal Cross-sections and Natural Abundances of Lithium and Boron.

ISOTOPE	THERMAL NEUTRON CROSS-SECTION	ENRICHMENT	NATURAL ABUNDANCE
^{6}Li	953 b	95-96%	7 %
^{7}Li	0.037 b	99.9%	93 %
^{10}B	3840 b	95-96%	20 %
^{11}B	0.005 b	99%	80 %

$Li_2B_4O_7$ can be made more sensitive to thermal neutrons by enriching it with ^6Li and ^{10}B. Thus, $^6Li_2{}^{10}B_4O_7$ is extremely sensitive to slow neutrons, while $^7Li_2{}^{11}B_4O_7$ is insensitive to neutrons. However, there is a very small probability that fast and epithermal neutrons will be captured by $^6Li_2{}^{10}B_4O_7$, but these neutrons can interact with a person's body and be scattered back toward the TLD. The result is that some of these fast and epithermal neutrons are moderated or slowed down and can be captured by the phosphor, $Li_2B_4O_7$. This albedo effect forms the basis for the Panasonic UD-809AS (Panasonic Industrial Company, 1989). Incidentally, the two phosphors of $Li_2B_4O_7$ have approximately the same sensitivity to gamma radiation.

3.6. Panasonic UD-802AS

The UD-802AS Panasonic dosimeter is a personnel TLD which measures both gamma and beta radiation. The TLD consists of four chips or elements. Two elements are $Li_2B_4O_7$ under 14 and 300 mg/cm^2 of plastic filters. The remaining two elements are $CaSO_4$: one under 300 mg/cm^2 of plastic and one under 1000 mg/cm^2 of plastic plus lead (Panasonic Industrial Company, 1989).

3.7. PMMA Phantom

In radiation exposures, phantoms are used to simulate the effect of the human body on incident radiation. Both phantoms and the human body cause incident radiation to backscatter which results in variations in energies and angular distributions. The American National Standards Institute (ANSI) recommends that phantoms be made of

polymethyl methacrylate or PMMA which gives similar scattering and dose distributions similar to tissue. The phantoms are a rectangular slab of face size 40 x 40 cm and a thickness of 15 cm. For neutron irradiations, the sensitive volume of the dosimeters should not be closer than 10 cm to the phantom's edge, and for gamma irradiations the sensitive volume should not be closer than 7.5 cm to the phantom's edge (ANSI N13.11, 1993).

CHAPTER IV

RESULTS

4.1 Supralinearity

The Panasonic UD-809AS and UD-802AS dosimeters are often used together in the 887 holder; thus, supralinearity measurements were completed for both dosimeters simultaneously. Because these dosimeters are normally worn against the body, a 40 x 40 x 15 PMMA phantom is used to simulate the human body in these measurements. D_2O-moderated californium-252 is used for supralinearity measurements primarily because the D_2O-moderated ^{252}Cf spectrum is well-known and is a softer spectrum which more resembles the spectrum that would be seen near a reactor (Schwartz and Eisenhauer, 1980). Another reason to use D_2O-moderated ^{252}Cf for supralinearity measurements is that the American National Standards Institute recommends this source configuration for neutron calibration testing (ANSI N13.11, 1993). Also, because of the recommended calibration distance for neutrons is 50 cm (ANSI N13.11, 1993), supralinearity measurements up to 100 rad are exposed at this distance. For doses in the range from 100 to 1000 rad, a decreased distance of 17 cm is used because of time constraints. The processing of the supralinearity measurements involved two different Panasonic readers: the UD-702E manual reader located at ORNL for doses up to 100 rad and the UD-710 automatic reader from the TVA Watts Bar facility from doses in the range of 100 to 1000

rad. The change in readers is necessary because at higher doses, the older manual reader has limited electronic capabilities.

Results of supralinearity measurements are found in Figures 2.8 and 2.9. These figures show that both the UD-809AS and the UD-802AS are linear at lower doses. Slopes in the linear region of these curves are found in Table 4.1. However, above approximately 10 rad, the TLD response begins to deviate from linearity. A curve fit is used to obtain a fit in this nonlinear region in the form of Equation 4.1.

$$mR^* = a + bD + cD^2 + dD^3 + eD^{1/2} \tag{4.1}$$

where mR^* = Element Response

D = Absorbed Dose

a, b, c, d, and e = coefficients to be determined

Coefficients, determined from TableCurve (Jandel Scientific TableCurve, 1991), are found for each element in Table 4.1 for the UD-809AS TLD and 4.2 for the UD-802AS TLD. By using Equation 4.1 with the appropriate coefficients, element responses can be corrected for doses from the range of 10 rad to 1000 rad.

4.2 Response Function Using Four Neutron Spectra

As described in Section 2.7, a linear combination of the Panasonic UD-809AS's elements can be used to obtain some spectral information in three energy groups for any spectrum. In order to determine the coefficients used in this linear combination, the fluence in each energy bin is found from each perspective spectrum (IAEA 318, 1990) and (Tanner, et al., 1994). A set of eight Panasonic UD-809AS dosimeters were

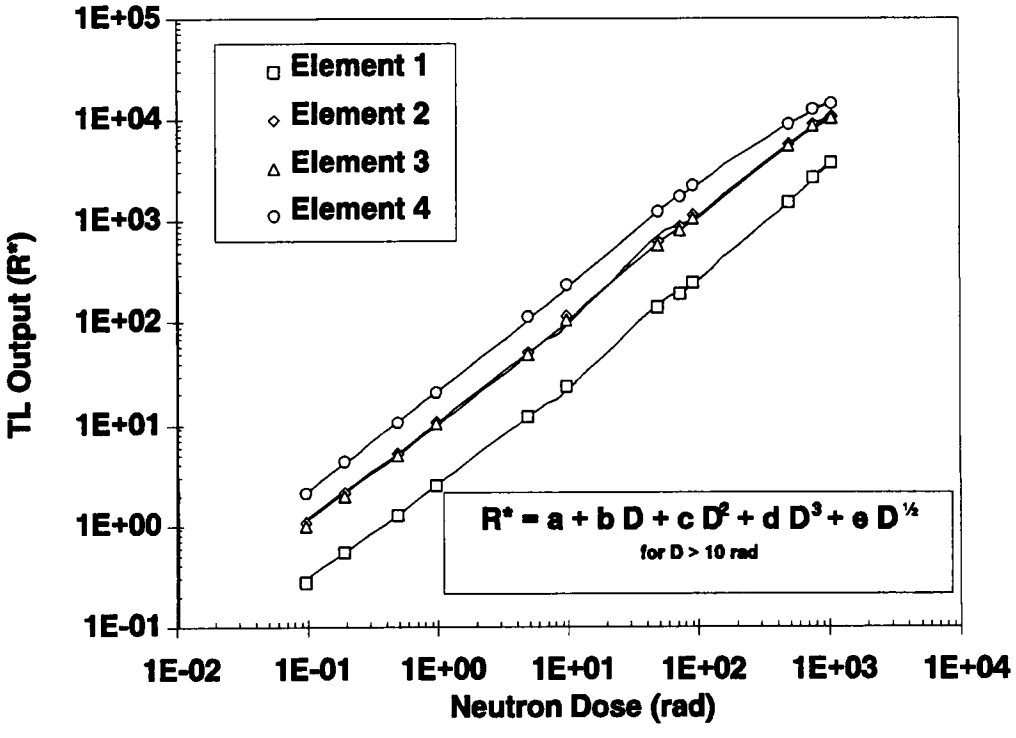


Figure 4.1 Panasonic UD-809AS Response to D_2O-Moderated ^{252}Cf.

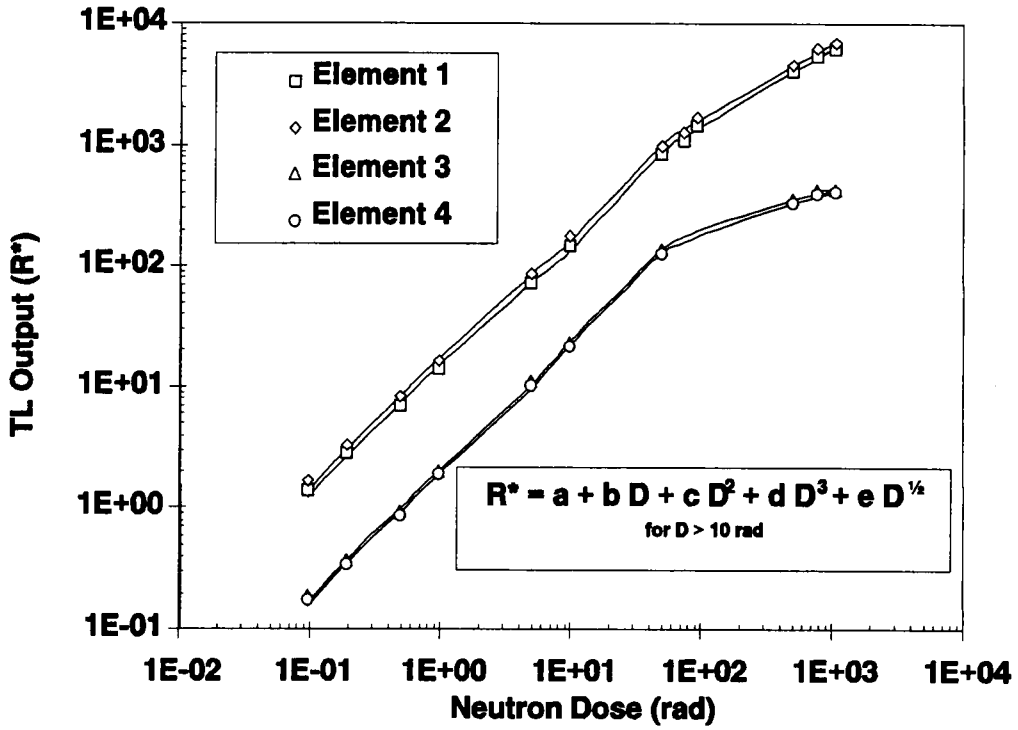


Figure 4.2 Panasonic UD-802AS Response to D_2O-Moderated ^{252}Cf.

Table 4.1 Results of Supralinearity Measurements for the UD-809AS Dosimeters.

Element Number	Slope (in linear region)	a	b	c	d	e
1 ($^{7}Li_2{}^{11}B_4O_7$)	2.53	-105.14	-1.80	8.36E-3	-4.27E-6	46.27
2 ($^{6}Li_2{}^{10}B_4O_7$)	10.52	-630.19	-13.34	4.03E-2	-2.42E-5	272.69
3 ($^{6}Li_2{}^{10}B_4O_7$)	10.06	-276.08	-0.38	2.00E-2	-1.27E-5	122.59
4 ($^{6}Li_2{}^{10}B_4O_7$)	22.36	-408.48	9.60	1.03E-2	-1.04E-5	173.28

Table 4.2 Results of Supralinearity Measurements for the UD-802AS Dosimeters.

Element Number	Slope (in linear region)	a	b	c	d	e
1 ($Li_2B_4O_7$)	15.26	-515.71	-2.46	6.00E-3	-3.60E-6	216.31
2 ($Li_2B_4O_7$)	18.09	-626.91	-4.64	9.48E-3	-5.59E-6	266.39
3 ($CaSO_4$)	2.11	-113.60	-2.05	2.02E-3	-9.98E-7	50.26
4 ($CaSO_4$)	1.98	-91.25	-1.35	1.06E-3	-4.85E-7	40.52

irradiated in four separate exposures to 500 mrem each to bare ^{252}Cf, D_2O-moderated ^{252}Cf, polyethylene-moderated ^{252}Cf, and ^{241}Am-Be. The dosimeters were read using the Panasonic UD-702E reader to get the element responses, X's, in units of mR^* after allowing 24 hours for initial fading to occur. At this point, the coefficients, α's, can be determined from Equation 2.30. The coefficients for each energy group are found in this manner and are reported in Table 4.3. These coefficients determine the fluence for any unknown spectrum and are applied by multiplying the given coefficient by the response of each element in the Panasonic UD-809AS dosimeter.

These coefficients have been tested by an exposing dosimeters to ^{238}Pu-Be. Four Panasonic UD-809AS dosimeters were exposed to 500 mrem of ^{238}Pu-Be at 50 cm on the PMMA phantom. The average response of each element is multiplied by the corresponding coefficient in each energy group. Then, the elements in each energy group are summed to get the fluence. The fractional true fluence (Block et al., 1967) and the fractional fluence determined with coefficients are found in Table 4.4.

4.3 Effects of Phantom

In neutron dosimetry, the phantom is very important because it simulates the human body and scatters radiation back towards the dosimeter. This back-scattering effect is very important for albedo dosimeters which often respond better to thermal neutrons than to fast neutrons. The idea of being able to correct the dosimeter response for an unphantomed measurement or exposure was proposed (Miller, 1994).

In order to correct dosimeter responses for unphantomed exposures for neutrons,

Table 4.3 Coefficients for Determining Fluence for Each Energy Group.

	thermal	epithermal	fast
α_1	-37,051	-126,267	408,945
α_2	109,088	19,920	-37,094
α_3	-70,708	102,291	-211,990
α_4	-12,803	-7,098	83,328

Table 4.4 Fractional Fluence for Energy Bins for ^{238}Pu-Be.

	True Fractional Fluence (Block et al., 1967)	Fractional Fluence Using Coefficients
thermal	0.0077	0.0083
epithermal	0.02698	0.0900
fast	0.9653	0.9017

measurements with and without the phantom must be made for various neutron sources. Panasonic UD-809AS and UD-802AS TLD's were exposed to three different neutron sources: bare ^{252}Cf, D_2O-moderated ^{252}Cf, and polyethylene-moderated ^{252}Cf. 500 mrem exposures were made at 50 cm. These exposures were made once on a phantom and once again in air. These two exposures (in air and on a phantom) allow for a correction to be made on dosimeter responses for unphantomed exposures. A Phantom Correction Factor (PCF) is determined for each spectrum by taking the ratio of these two measurements as seen in Equation 4.2.

$$PCF = \frac{mR^{*}_{\text{on a phantom}}}{mR^{*}_{\text{in air}}} \tag{4.2}$$

The Phantom Correction Factors are found in Table 4.5 and 4.6. As can be seen by examining the PCFs, the PMMA phantom has a very significant effect on the Panasonic's TLDs response. The PCFs for the neutron elements of the Panasonic UD-802AS and the UD-809AS vary from 1.120 to 5.081. Thus, as would be expected, the PMMA phantom which simulates the human body is very important in neutron dosimetry.

Table 4.5 Phantom Correction Factors for Panasonic UD-809AS.

Element	PCF	Spectra
2	1.837	D_2O-moderated
2	2.564	Bare ^{252}Cf
2	1.120	Polyethylene-moderated
3	1.909	D_2O-moderated
3	1.787	Bare ^{252}Cf
3	1.309	Polyethylene-moderated
4	3.542	D_2O-moderated
4	4.818	Bare ^{252}Cf
4	2.341	Polyethylene-moderated

Table 4.6 Phantom Correction Factors for Panasonic UD-802AS.

Element	PCF	Spectra
1	5.081	D_2O-moderated
1	2.504	Bare ^{252}Cf
1	1.460	Polyethylene-moderated
2	4.744	D_2O-moderated
2	3.016	Bare ^{252}Cf
2	1.509	Polyethylene-moderated

CHAPTER V

CONCLUSIONS AND FUTURE WORK

Lithium tetraborate, enriched in the isotopes of ^{6}Li and ^{10}B as used in the Panasonic UD-809AS dosimeter, is an acceptable material for measuring neutron doses associated with a criticality accident in the range of 1 to 1000 rad after correcting for the effects of supralinearity above 10 rad. The UD-809AS dosimeter can also be used in a variety of neutron fields with appropriate Spectral Correction Factors (SCFs) for 115 accident spectra. The SCFs correct the response of the UD-809AS for variations caused by different spectra. The results of the SCFs should be improved further by taking into consideration the effects of the phantom on the accident spectra. As seen from the Phantom Correction Factors, the PMMA phantom, as well as the human body, has a significant effect on the Panasonic dosimeters' responses. Also, some spectral information in limited energy bins (thermal, epithermal, and fast) is currently available by using this dosimeter in a linear combination to four sources.

Future work for the Panasonic UD-809AS dosimeter to be used as an accident personnel dosimeter should include supralinearity measurements in a gamma field in the range of 10 to 1000 rad and verification of gamma and neutron doses in an accident scenario by using a well characterized reactor.

BIBLIOGRAPHY

BIBLIOGRAPHY

Alevra, A. V.; Cosack, M.; Hunt, J. B.; Thomas, D. J.; Schraube, H. S. Experimental Determination of the Response of Four Bonner Sphere Sets to Monoenergetic Neutrons. Rad. Prot. Dos. 40: 91-101; 1992.

American National Standards Institute. American National Standard Dosimetry for Criticality Accidents. ANSI N13.3; 1976.

American National Standards Institute. American National Standard for Dosimetry - Personnel Dosimetry Performance - Criteria for Testing. ANSI N13.11; 1993.

American National Standards Institute. American National Standard for Personnel Neutron Dosimeters (Neutron Energies Less than 20 MeV). ANSI N319; 1976.

American National Standards Institute. American National Standard for Radiation Detectors - Personnel Thermoluminescence Dosimetry Systems - Performance. ANSI N13.15; 1985.

Aroua, A.; Grecescu, M.; Lerch, P.; Pretre, S.; Valley, J. F. A Rapid Way to Process Bonner Spheres Data. Rad. Prot. Dos. 46: 45-8; 1993.

Aroua, A.; Grecescu, M.; Lanfranchi, M.; Lerch, P.; Pretre, S,; Valley, J. F. Evaluation and Test of the Response of a Multisphere Neutron Spectrometer in a Wide Energy Range: Part II Simulation. Nucl. Instr. Meth. A321: 305-11; 1992.

Aroua, A.; Grecescu, M.; Lerch, P.; Pretre, S,; Valley, J. F. Evaluation and Test of the Response Matrix of a Multisphere Neutron Spectrometer in a Wide Energy Range: Part III Validation. Nucl. Instr. Meth. A321: 312-6; 1992.

Block, S.; Bryan, J.; Prevo, C.; Montan, D. Laboratory Sources Enhanced in 0.5 eV to 200 keV Neutrons for Instrument Evaluation. Health Phys. 13: 1025-1031; 1967.

Brackenbush, L. W.; Baumgartner, W. V.; Fix, J. J. Response of TLD-Albedo and Nuclear Track Dosimeters Exposed to Plutonium Sources Appendix B. Richland: Pacific Northwest Laboratory; PNL-7881/UC-606; December 1991.

Buckner, M. A.; Sims, C. S. Neutron Dosimetric Quantities for Several Radioisotopic Neutron Sources. Health Phys. 63: 352-5; 1992.

Burgkhardt, B.; Piesch, E.; Singh, D. High-dose Characteristics of LiF and $Li_2B_4O_7$ Thermoluminescent Dosimeters. Nucl. Instr. Meth. 148: 613-7; 1978.

Burgkhardt, B.; Singh, D.; Piesch E. High-dose Characteristics of CaF_2 and $CaSO_4$ Thermoluminescent Dosimeters. Nucl. Instr. Meth. 141: 363-8; 1977.

Casson, W. H.; Mei, G. T.; Buckner, M. A. Test and Recommendations for the Application of the Centralized External Dosimetry System Dosimeter to Nuclear Accident Dosimetry. Oak Ridge: Oak Ridge National Laboratory; ORNL-6667; September 1993.

Chen, R.; Fogel, G. Superlinearity in Thermoluminescence Revisited. Rad. Prot. Dos. 47: 23-6;1993.

Davy, D. R.; O'Brien, B. G. An Adapted Model for the LET Dependence of LiF Thermoluminescence. Health Phys. 17: 471-82; 1969.

Delafield, H. J. Nuclear Accident Dosimetry - An Overview. Rad. Prot. Dos. 23: 143-9; 1988.

Delafield, H. J.; Dennis, J. A.; Gibson, J. A. B. Nuclear Accident Dosimetry: Part I General Principles. Harwell: National Radiological Protection Board; AERE - R 7485; November 1973.

Delafield, H. J.; Dennis, J. A.; Gibson, J. A. B. Nuclear Accident Dosimetry: Part II Dose Assessment Procedure. Harwell: National Radiological Protection Board; AERE - R 7486; November 1973.

Delafield, H. J.; Dennis, J. A.; Gibson, J. A. B. Nuclear Accident Dosimetry: Part III Interpretation and Data. Harwell: National Radiological Protection Board; AERE - R 7487; December 1973.

Duderstadt, J. J.; Hamilton L. J. Nuclear Reactor Analysis. New York: John Wiley & Sons; 1976.

Eisenhauer, C. M.; Hunt J. B.; Schwartz, R. B. Calibration Techniques for Neutron Personnel Dosimetry. Rad. Prot. Dos. 10: 43-57; 1985.

Eisenhauer, C. M.; Schwartz, R. B.; McCall R. C. Effect of Air Scatter on Calibration of Instruments for Detecting Neutrons. Rad. Prot. Dos. 19: 77-84; 1987.

Eisenhauer, C. M. Evaluation of Dose Equivalent Per Unit Fluence for a D_2O-Moderated ^{252}Cf Neutron Source. Rad. Prot. Dos. 9: 63-4; 1984.

Eisenhauer, C. M.; Schwartz, R. B.; Johnson, T. Measurement of Neutrons Reflected from the Surfaces of a Calibration Room. Health Phys. 42: 489-95; 1982.

Eisenhauer, C. M. Review of Scattering Corrections for Calibration of Neutron Instruments. Rad. Prot. Dos. 28: 253-62; 1989.

Eisenhauer, C. Two-Component Analytical Model to Calculate Room-Return Correction for Calibration of Neutron Instruments. Rad. Prot. Dos. 42: 267-77; 1992.

Frame, P. W. Thermoluminescent Dosimetry: Class Notes. 1993.

Furuta, Y.; Tanaka, S. Response of ^{6}LiF and ^{7}LiF Thermoluminescence Dosimeters to Fast Neutrons. Nucl. Instr. Meth. 104: 365-74; 1972.

Hahn, T.; Fellinger, J.; Hubner, K.; Schmidt, P. Neutron Response of LiF TL Detectors. Rad. Prot. Dos. 44: 297-300; 1992.

Hajnal, F. Technique for Determining Moderated-Neutron Instrument Characteristics. New York: U.S. Atomic Energy Commission; 1970.

Henniger, J.; Hubner, K.; Pretzsch, G. Calculation of the Neutron Sensitivity of TL Detectors. Nucl. Instr. Meth. 192: 453-62; 1982.

Hertel, N. E; Davidson, J. W. The Response of Bonner Spheres to Neutrons from Thermal Energies to 17.3 MeV. Nucl. Instr. Meth. A238: 509-16; 1985.

Hertel, N. E. Calculations of Anisotropy Factors and Dose Equivalents for Unmoderated ^{252}Cf Sources. Rad. Prot. Dos. 32: 77-82; 1990.

Horowitz, Y. S. Mathematical Modelling of TL Supralinearity for Heavy Charged Particles. Rad. Prot. Dos. 33: 75-81; 1990.

Horowitz, Y. S. Thermoluminescence and Thermoluminescent Dosimetry, Volume I, II, and III. Boca Raton: CRC Press; 1984.

International Atomic Energy Agency. Compendium of Neutron Spectra and Detector Responses for Radiation Protection Purposes. Vienna: IAEA; Technical Reports Series Number 318: 1-274; 1990.

International Atomic Energy Agency. Compendium of Neutron Spectra in Criticality Accident Dosimetry. Vienna: IAEA; Technical Reports Series Number 180: 1-193; 1978.

International Atomic Energy Agency. Dosimetry for Criticality Accidents. Vienna: IAEA; 1982.

International Atomic Energy Agency. Neutron Monitoring for Radiological Protection. Vienna: IAEA; Technical Reports Series Number 252: 1-222; 1985.

International Commission on Radiological Protection. Data for Protection against Ionizing Radiation from External Sources: Supplement to ICRP Publication 15. Oxford: Pergamon Press; ICRP Publication 21; 1-101; 1971.

International Organization for Standardization. Neutron Reference Radiations for Calibrating Neutron Measuring Devices Used for Radiation Protection Purposes and for determining Their Response as a Function of Neutron Energy. ISO/DIS 8529; 1986.

Jandel Scientific TableCurve. Version 3.01; 1991.

Kaplan, I. Nuclear Physics. Second Edition. Reading, MA: Addison-Wesley Publishing Company; 1962.

Kluge, H.; Weise K.; Hunt, J. B. Calibration of Neutron Sensitive Spherical Devices with Bare and D_2O Moderated ^{252}Cf Sources in Rooms of Different Sizes. Rad. Prot. Dos. 32: 233-44; 1990.

Knoll, G. F. Radiation Detection and Measurement. Second Edition. New York: John Wiley & Sons; 1989.

Larson, L.; Katz, R. Supralinearity of Thermoluminescent Dosimeters. Nucl. Instr. Meth. 138: 631-6; 1976.

Lemley, E. C. Neutron Spectra Characterization with the Bonner Sphere Detection System: A Thesis. University of Arkansas; December, 1991.

Luzszik-Bhadra, M.; Alberts, W. G.; Dietz, E.; Guldbakke, S. Aspects of Combining Albedo and Etched Track Techniques for Use in Individual Neutron Monitoring. Rad. Prot. Dos. 46: 31-6; 1993.

McKeever, S. W. S. Modeling Supralinearity in Gamma Irradiated TL Dosemeters. Rad. Prot. Dos. 33: 83-9; 1990.

Mares, V.; Schraube, G.; Schraube, H. Calculated Neutron Response of a Bonner Sphere Spectrometer with ^{3}He Counter. Nuc. Instr. Meth. A307: 398-412; 1991.

Marinkovic, P.; Avdic S.; Pesic, M.; Zavalijevski, N. The Effect of the Neutron Spectra Unfolding Method on the Fast Neutron Dose Determination. Nucl. Instr. Meth. A321: 333-5; 1992.

Miller, L. F. Private communication, 1993.

Miller, L. F. Private communication, 1994.

Mische, E. F.; McKeever, S. W. S. Mechanisms of Supralinearity in Lithium Fluoride Thermoluminescence Dosemeters. Rad. Prot. Dos. 29: 159-75; 1989.

Oak Ridge National Laboratory. Radiation Calibration Laboratory Protocol. Oak Ridge; DOSAR Report No. 1-91; December 1991.

O'Brien, K.; Sanna, R. Neutron Spectral Unfolding Using the Monte Carlo Method. Nucl. Instr. Meth. 185: 277-86; 1981.

Panasonic Industrial Corporation. User's Manual for the Panasonic UD-710 Automatic TLD Reader and the UD-702 Manual TLD Reader. November 1989.

Perks C. A.; Thomas D. J.; Siebert B. R. L.; Jetzke, S.; Hehn, G.; Schraube, H. Comparison of Response Function Calculations for Multispheres. Rad. Prot. Dos. 44: 85-9; 1992.

Piesch, E.; Burgkhardt, B.; Kabadjova, S. Supralinearity and Re-evaluation of Different LiF Dosimeter Types. Nucl. Instr. Meth. 126: 563-72; 1975.

Pulpan, J.; Kralik, M. Geometrical Correction Factor. Rad. Prot. Dos. 35: 159-65; 1991.

Reddy, A. R.; Metha, S. C. Dosimetry of Very Low Energy Photons. Health Phys. 36: 175-82; 1979.

Santoro, R. T.; Alsmiller, R. J. Jr; Barnes, J. M. Nuclear Accident Dosimetry: Calculations and Comparisons with Experimental Data. Health Phys. 36: 189-91; 1979.

Siebert, B. R. L.; Dietz E.; Jetzke, S. Comparison of Measured and Calculated Bonner Sphere Responses for 24 and 144 keV Incident Neutron Energies. Rad. Prot. Dos. 44: 89-92; 1992.

Siebert, B. R. L.; Morhart, A. A Proposed Procedure for Standardizing the Relationship between the Directional Dose Equivalent and Neutron Fluence. Rad. Prot. Dos. 28: 47-51; 1989.

Schuhmacher, H.; Alberts, W. G. Reference Neutron Fields with Energies up to 70 MeV for the Calibration of Radiation Protection Instruments. Rad. Prot. Dos. 42: 287-290; 1992.

Schmidt, P.; Fellinger, J.; Hubner, K. Experimental Determination of the TL Response for Protons and Deuterons in Various Detector Materials. Rad. Prot. Dos. 33: 171-3; 1990.

Schwartz, R. B. Private communication, 1993.

Schwartz, R. B.; Eisenhauer, C. M. Procedures for Calibrating Neutron Personnel Dosimeters. Washington, D. C.: National Bureau of Standards; May 1982.

Schwartz, R. B.; Eisenhauer, C. M. The Design and Construction of a D_2O-Moderated ^{252}Cf Source for Calibrating Neutron Personnel Dosimeters Used at Nuclear Power Reactors. Washington, D. C.: National Bureau of Standards; NUREG/CR-1204; January 1980.

Sims, C. S. Nuclear Accident Dosimetry Intercomparison Studies. Health Phys. 57: 439-48; 1989.

Sims, C. S.; Dickson, H. W. Nuclear Accident Dosimetry Intercomparison Studies at the Health Physics Reactor: A Summary (1965-1978). Health Phys. 37: 687-99; 1979.

Snapp, J. P. Development of a Neutron Area Monitor and Characterization System: A Thesis. University of Tennessee, Knoxville; December 1992.

Spurny, F.; Medioni, R.; Portal, G. Energy Transfer to Some TLD Materials by Neutrons: Comparison of Theoretical and Experimental Data. Nucl. Instr. Meth. 138: 165-71; 1976.

Takenaga, M.; Yamaoto, O. Yamshita, T. Preparation and Characteristics of $Li_2B_4O_7$:Cu Phosphor. Nucl. Instr. Meth. 175: 77-8; 1980.

Tanaka, S.; Furuta, Y. Revised Energy Responses of ^6LiF and ^7LiF Thermoluminescence Dosimeters to Neutrons. Nucl. Instr. Meth. 140: 395-6; 1977.

Tanaka, S.; Furuta, Y. Usage of a Thermoluminescence Dosimeter As a Thermal Neutron Detector with High Sensitivity. Nucl. Instr. Meth. 133: 495-9; 1976.

Tanner, J. E.; Casson, W. H.; Soldat, K. L.; Stewart, R. D. Fluence-to-Dose Equivalent Conversion Factors for Polyethylene-Moderated ^{252}CF. 1994.

Thompson, J. J.; Ziemer, P. L. Energy Response of Lithium Borate Thermoluminescent Dosimeters. Health Phys. 22: 399-401; 1972.

Turner, J. E. Atoms, Radiation, and Radiation Protection. First printing. New York: Pergamon Press; 1986.

U.S. Department of Energy. Radiation Protection for Occupational Workers. Washington, DC; 1988.

U.S. Nuclear Regulatory Commission. Code of Federal Regulation. Washington, DC: U.S. Government Printing Office; 10 CFR Part 70; 19?.

U.S. Nuclear Regulatory Commission. Code of Federal Regulation. Washington, DC: U.S. Government Printing Office; 10 CFR Part 835; 1993.

Walker, F. W.; Parrington, J. R.; Feiner, F. eds. Nuclides and Isotopes. Fourteenth Edition. San Jose, CA: General Electric Company; 1989.

Wasek, P. N. Private communication, 1994.

Zaidins, C. S.; Martin, J. B.; Edwards, M. E. A Least-Squares Technique for Extracting Neutron Spectra from Bonner Sphere Data. Med. Phys. 5:42-7; 1978.

APPENDICES

APPENDIX A

DATA

A.1 Data from ECF Exposures

Table A.1.1 TLD Readings in Units of mR* for Reference Group Exposed to 500 mR of Cesium-137 for ECF Calculation.

ID Number	Element 1	Element 2	Element 3	Element 4
UD-809AS				
2	300	328	333	298
6	267	380	352	351
8	283	336	312	337
27	293	412	401	412
45	257	308	311	326
58	264	312	343	319
61	273	272	346	257
UD-802AS				
618	563	455	358	420
715	514	462	442	495
758	583	471	365	429
828	509	450	424	506
857	543	486	444	483
858	576	465	417	478
918	504	452	404	457
993	492	458	459	528

ID Number	Element 1	Element 2	Element 3	Element 4
996	548	466	444	507
1068	588	514	475	509
1092	491	457	410	525
1214	576	490	475	526
1225	529	450	461	528
1258	514	465	436	486
1291	597	509	474	530
1306	569	476	432	480
1374	608	498	486	576
1392	540	480	460	516
1448	494	421	414	474
1460	555	484	464	525

Table A.1.2 TLD Readings in Units of mR* for Reference Group Exposed to 500 mR of Cesium-137 for ECF Calculation.

ID Number	Element 1	Element 2	Element 3	Element 4
UD-809AS				
2	299	333	317	297
6	269	359	334	343
8	295	330	315	317
27	293	399	397	394
45	245	298	305	301
58	259	302	347	311
61	264	262	344	270
UD-802AS				
618	584	441	354	420
715	503	467	443	494
758	578	464	366	442
828	514	442	409	508
857	568	483	445	490
858	568	445	416	476
918	516	460	402	458
993	489	437	454	529
996	537	472	437	509
1068	614	512	479	509
1092	491	454	410	522
1214	557	503	473	524
1225	529	467	452	532
1258	520	454	445	489
1291	587	496	474	529

ID Number	Element 1	Element 2	Element 3	Element 4
1306	578	488	433	484
1374	625	492	491	577
1392	511	487	466	508
1448	498	426	411	475
1460	530	482	462	519

Table A.1.3 TLD Readings in Units of mR* for Reference Group Exposed to 500 mR of Cesium-137 for ECF Calculation.

ID Number	Element 1	Element 2	Element 3	Element 4
UD-809AS				
2	297	336	351	299
6	268	380	352	362
8	296	335	333	330
27	314	402	397	408
45	250	317	311	333
58	271	311	354	325
61	266	287	354	276
UD-802AS				
618	616	448	357	411
715	519	474	448	505
758	596	472	367	433
828	525	446	414	499
857	565	482	454	492
858	611	460	419	487
918	531	475	404	457
993	496	461	454	528
996	567	442	435	503
1068	630	512	480	511
1092	501	479	409	517
1214	575	516	472	532
1225	515	452	456	530
1258	535	468	448	503
1291	584	495	488	531

ID Number	Element 1	Element 2	Element 3	Element 4
1306	596	497	435	492
1374	649	501	490	584
1392	528	500	452	514
1448	485	423	413	483
1460	549	492	481	521

Table A.1.4 TLD Readings in Units of mR* for Non-Reference Group Exposed to 500 mR of Cesium-137 for ECF Calculation.

ID Number	Element 1	Element 2	Element 3	Element 4
UD-809AS				
3	257	338	306	333
4	239	314	316	356
5	237	292	330	276
10	226	285	284	296
11	242	297	312	290
12	244	321	339	293
14	178	268	282	272
15	269	300	302	298
16	221	302	327	280
17	230	297	316	293
18	222	310	326	263
19	261	330	350	388
20	273	344	334	347
21	285	326	333	350
22	314	312	351	350
23	234	275	331	311
25	271	323	330	277
26	268	294	293	279
28	291	339	336	347
29	265	329	328	289
30	251	322	333	308
31	285	341	331	344
32	308	375	340	364

ID Number	Element 1	Element 2	Element 3	Element 4
33	336	374	330	347
34	262	302	351	305
35	268	328	345	317
37	297	383	348	332
38	272	324	350	297
39	321	364	398	365
40	271	388	365	344
41	247	296	283	305
42	278	327	334	321
43	280	293	304	305
44	293	329	337	327
47	307	303	303	286
48	234	318	308	342
49	234	316	293	296
50	291	280	306	284
51	295	290	306	295
53	259	285	295	275
54	278	286	322	291
55	302	340	322	336
57	317	385	338	366
60	260	286	268	271
62	255	305	354	293
63	233	293	310	285
64	303	333	330	326
65	298	290	281	296
71	268	277	313	282

ID Number	Element 1	Element 2	Element 3	Element 4
UD-802AS				
603	526	436	360	390
623	516	441	346	359
629	535	448	343	384
643	556	456	354	421
676	496	470	420	471
683	477	419	411	480
701	519	434	409	486
718	506	476	395	448
723	532	423	425	451
737	489	432	381	472
742	468	418	415	451
746	551	503	433	499
751	584	490	342	392
770	545	447	355	387
773	540	461	370	411
774	468	422	323	365
777	548	416	364	401
818	519	458	405	459
820	487	453	417	459
825	540	430	397	466
838	567	463	440	423
840	509	455	409	462
855	529	444	434	470
895	555	449	416	499
920	526	447	394	460

ID Number	Element 1	Element 2	Element 3	Element 4
962	470	422	435	482
965	556	514	426	482
968	570	448	399	486
971	473	408	470	520
989	524	449	427	484
1006	542	470	448	495
1012	521	457	472	492
1014	501	454	450	508
1025	574	509	410	454
1028	552	448	420	486
1032	576	448	475	466
1048	483	459	420	502
1053	599	497	467	542
1070	526	410	475	542
1078	570	511	485	539
1079	536	443	486	539
1081	606	503	439	519
1100	502	404	414	430
1110	580	461	417	464
1112	548	442	434	472
1116	493	448	462	483
1118	517	440	446	508
1125	533	498	422	467
1129	539	490	445	496
1137	524	441	400	444
1165	515	407	473	482

ID Number	Element 1	Element 2	Element 3	Element 4
1171	457	465	488	502
1176	520	453	420	447
1192	558	496	423	479
1201	496	413	458	520
1241	585	519	484	527
1245	585	510	444	528
1254	502	468	462	502
1255	504	411	421	489
1257	484	462	447	474
1260	512	481	443	482
1262	536	491	434	495
1301	530	409	452	479
1302	557	432	456	505
1311	471	458	435	471
1319	508	460	439	495
1355	494	487	467	528
1356	541	466	482	513
1359	557	462	455	513
1367	513	437	442	489
1398	511	467	457	554
1432	489	442	442	481
1434	492	431	455	487
1452	510	472	454	423
1461	520	469	437	481
1468	527	465	497	527
1469	575	500	470	507

ID Number	Element 1	Element 2	Element 3	Element 4
1471	470	461	473	491
1474	500	452	469	524
1486	524	439	452	492

Table A.1.5 TLD Readings in Units of mR* for Reference Sub-Group Exposed to 500 mR of Cesium-137 for ECF Calculation.

ID Number	Element 1	Element 2	Element 3	Element 4
UD-809AS				
6	274	362	340	354
8	299	334	325	336
UD-802AS				
858	593	469	412	486
918	522	467	397	454
993	496	454	443	514
1068	615	520	474	505
1258	537	472	434	486
1448	491	435	405	478

Table A.1.6 TLD Readings in Units of mR* for Non-Reference Group Exposed to 500 mR of Cesium-137 for ECF Calculation.

ID Number	Element 1	Element 2	Element 3	Element 4
UD-809AS				
1801	316	285	292	292
1802	271	286	276	241
1803	263	243	249	254
1804	260	270	248	258
1805	286	272	310	294
1806	282	283	283	273
1807	247	287	268	291
1808	309	262	298	269
1809	324	289	274	274
1810	288	275	239	260
1811	285	262	258	262
1812	280	271	268	258
1813	275	278	295	257
1814	250	281	227	252
2800	262	262	293	272

Table A.1.7 TLD Readings in Units of mR* for Reference Sub-Group Exposed to 500 mR of Cesium-137 for ECF Calculation.

ID Number	Element 1	Element 2	Element 3	Element 4
UD-809AS				
6	258	340	313	338
8	301	321	298	336
UD-802AS				
858	566	468	468	545
918	495	440	444	518
993	515	457	515	586
1068	593	504	539	568
1258	514	453	490	556
1448	474	389	454	531

Table A.1.8 TLD Readings in Units of mR* for Non-Reference Group Exposed to 500 mR of Cesium-137 for Justification for Using Only One Irradiation for Non-Reference ECF Calculation.

ID Number	Element 1	Element 2	Element 3	Element 4
UD-809AS				
20	240	312	304	310
30	224	294	292	299
37	280	438	313	315
65	285	263	264	280
UD-802AS				
968	621	501	412	506
1137	570	501	414	470
1260	572	538	463	504
1486	588	502	469	512

Table A.1.9 TLD Readings in Units of mR* for Reference Sub-Group Exposed to 500 mR of Cesium-137 for Justification for Using Only One Irradiation for Non-Reference ECF Calculation.

ID Number	Element 1	Element 2	Element 3	Element 4
UD-809AS				
6	234	315	297	309
8	287	325	289	321
UD-802AS				
858	627	510	447	515
918	535	481	414	477
993	538	500	480	557
1068	682	565	514	544
1258	582	517	468	520
1448	508	438	428	508

A.2 Data for Neutron and Gamma Equivalence

Table A.2.1 TLD Readings in Units of mR* for Exposure of 500 mR of Cesium-137 for Calculation of Cesium Equivalence.

ID Number	Element 1	Element 2	Element 3	Element 4
UD-809AS				
12	213	311	313	285
14	169	274	264	263
63	230	285	296	277
1813	251	251	252	249
UD-802AS				
742	415	473	498	509
962	435	498	535	544
1006	497	546	581	595
1468	463	490	613	621
Background Dosimeters				
UD-809AS				
53	15.4	23.6	21.2	33.7
1806	9.5	15.9	22.5	17.5
UD-802AS				
623	36.1	36.3	2.7	1.9
770	21.8	29.4	2.6	3.4

Table A.2.2 TLD Readings in Units of mR* for 500 mrem Exposure to D_2O-Moderated Californium-252 for Calculation of D_2O Equivalence.

ID Number	Element 1	Element 2	Element 3	Element 4
UD-809AS				
12	76.3	430	441	769
14	54.2	364	369	746
53	89.8	401	395	726
1803	86.8	351	365	697
UD-802AS				
770	835	838	80.1	77.8
1006	807	890	104	102
1245	878	969	104	110
1468	792	870	121	111
Backgrounds				
UD-809AS				
17	11	16.7	18.9	16.7
30	15.5	32.2	23.9	24.9
1802	8.8	13.7	15.8	11.8
UD-802AS				
629	18.2	22	4	4.4
746	70.9	53.7	0.3	0.4
1398	28.7	29.3	1.9	1.6

A.3 Data for Response Function Using Four Neutron Spectra

Table A.3.1 TLD Readings in Units of mR* for 500 mrem Exposure to D_2O-Moderated Californium-252 for Combination of Four Sources.

ID Number	Element 1	Element 2	Element 3	Element 4
UD-809AS				
33	109	463	475	881
35	84.6	452	443	822
40	85.7	503	470	866
50	92.4	373	411	749
51	100	418	410	831
53	82.7	378	404	737
1805	86.8	371	432	876
1810	86.9	365	337	724
UD-802AS				
701	822	880	105	103
770	859	870	84.3	82.2
838	855	858	110	94.1
855	806	853	107	98.2
1110	1130	981	108	103
1125	833	973	105	98.7
1192	842	935	99.8	100
1468	684	752	115	107
Background Dosimeters				
UD-809AS				
62	22.1	69.1	43.6	38.8
1801	14.8	17.1	23.4	15.1
1804	10.7	16.6	18.8	14.7

ID Number	Element 1	Element 2	Element 3	Element 4
UD-802AS				
920	22.8	25.3	2.5	2.4
1028	43.8	43.9	1.3	1.7
1359	33.6	34.9	3.7	3.5

Table A.3.2 TLD Readings in Units of mR* for 500 mrem Exposure to Bare Californium-252 for Combination of Four Sources.

ID Number	Element 1	Element 2	Element 3	Element 4
UD-809AS				
33	32.8	57.9	55.2	118
35	29.2	62.6	59.5	105
40	28.7	63.8	59.1	111
50	29.9	52.3	57.1	107
51	33	54.9	51.9	104
53	27.7	54	47.6	91.7
1805	26.2	45.5	55	104
1810	29.7	43.1	45.6	83.6
UD-802AS				
701	133	149	31.4	32.1
770	126	126	26.7	25.9
838	138	143	36	28.5
855	133	142	35.9	33.3
1110	155	158	33.8	33.5
1125	131	152	31.5	29.2
1192	144	148	31.3	30.1
1468	141	149	39.6	34.4
Background Dosimeters				
UD-809AS				
62	15.7	52.6	31.8	32.3
1801	11.5	14.5	18	10.8
1804	8.5	13.6	19.5	10.9

ID Number	Element 1	Element 2	Element 3	Element 4
UD-802AS				
920	22.1	19.5	1.5	1.3
1028	41.7	40.5	1.5	1.3
1359	26.1	28.7	2.3	2.4

Table A.3.3 TLD Readings in Units of mR* for 500 mrem Exposure to Americium-Beryllium for Combination of Four Sources.

ID Number	Element 1	Element 2	Element 3	Element 4
UD-809AS				
33	33.5	60.1	53.7	100
35	25.9	65.4	56.5	87.4
40	30.7	63.8	55.2	93.6
50	32.7	50.4	47.7	71.3
51	35.7	53.9	51.2	86.5
53	32.3	58.8	53.4	78.5
1805	26.4	41.8	58	83.9
1810	28.4	41.3	44	71.9
UD-802AS				
701	267	284	1900	363
770	234	226	1290	254
838	258	253	1920	267
855	229	231	1420	269
1110	282	255	1190	247
1125	210	247	1270	249
1192	281	295	1870	338
1468	232	239	1500	278
Background Dosimeters				
UD-809AS				
62	13.5	59.2	33	29.1
1801	8.1	14.5	15.3	9
1804	7.7	11.7	15.1	9.2

ID Number	Element 1	Element 2	Element 3	Element 4
UD-802AS				
920	22.2	17.6	1	1.1
1028	37.8	41.7	1.1	1.1
1359	28.6	29.1	2	1.7

Table A.3.4 TLD Readings in Units of mR* for 500 mrem Exposure to Polyethylene-Moderated Californium-252 for Combination of Four Sources.

ID Number	Element 1	Element 2	Element 3	Element 4
UD-809AS				
35	135	762	271	457
40	125	817	278	473
50	141	566	267	455
51	142	679	254	443
53	122	620	236	416
1805	126	577	249	463
1810	136	542	206	392
UD-802AS				
701	1120	1030	255	203
770	1090	1010	216	165
838	1170	1040	284	184
855	1040	1020	279	211
1110	1520	1150	268	208
1125	1210	1230	280	206
1192	1060	1070	251	201
1468	979	959	317	243
Background Dosimeters				
UD-809AS				
1801	6.8	12.2	13.3	9.1
1804	5.6	11.2	15.2	8.3

ID Number	Element 1	Element 2	Element 3	Element 4
UD-802AS				
920	20.7	14.7	0.8	0.8
1028	32.4	37.7	0.8	0.8
1359	21.5	23.8	1.2	1.2

Table A.3.5 TLD Readings in Units of mR* for 500 mrem Exposure to Plutonium-Beryllium for Verification of Combination of Four Sources Technique.

ID Number	Element 1	Element 2	Element 3	Element 4
UD-809AS				
12	24.9	50.5	51.8	70.6
14	17.2	49.1	54.2	79.3
64	28.9	61.1	58.7	102
1803	24.8	40.4	42.1	70.7
UD-802AS				
746	137	130	42.3	28.6
751	119	127	35.7	25.9
1245	126	131	41.9	31.7
1434	104	106	48.8	34.2
Background dosimeters				
UD-809AS				
1812	13.3	20.4	22	16.1
1814	10.3	18.1	17.2	15.7
UD-802AS				
1006	49.1	59.6	0.7	0.9
1079	28.9	30.5	8	8.7

A.4 Data for Supralinearity Measurements

Table A.4.1 TLD Readings in Units of R* for Dosimeters Exposed to 1 rem (0.097 rad) of D_2O-Moderated ^{252}Cf.

ID Number	Element 1	Element 2	Element 3	Element 4
UD-809AS				
15	0.164	0.716	0.737	1.45
19	0.173	0.798	0.87	1.8
23	0.137	0.658	0.823	1.57
34	0.157	0.77	0.89	1.62
48	0.138	0.79	0.787	1.64
57	0.307	1.03	0.821	1.81
60	0.173	0.74	0.693	1.35
71	0.147	0.705	0.775	1.34
UD-802AS				
643	1.76	1.85	0.167	0.176
773	1.8	1.98	0.169	0.166
989	1.5	1.61	0.192	0.207
1053	1.78	1.92	0.238	0.254
1081	1.72	1.87	0.203	0.218
1129	1.58	1.93	0.206	0.201
1262	1.6	1.79	0.197	0.202
1367	1.51	1.66	0.202	0.198
Background				
UD-809AS				
14	0.0174	0.0265	0.029	0.0283
30	0.0221	0.0303	0.0299	0.0306

ID Number	Element 1	Element 2	Element 3	Element 4
UD-802AS				
746	0.0543	0.0613	0.0053	0.0064
1006	0.0469	0.0565	0.0082	0.0094

Table A.4.2 TLD Readings in Units of R* for Dosimeters Exposed to 2 rem (0.193 rad) of D_2O-Moderated ^{252}Cf.

ID Number	Element 1	Element 2	Element 3	Element 4
UD-809AS				
15	0.302	1.42	1.48	2.97
19	0.286	1.54	1.68	3.79
23	0.253	1.32	1.6	3.11
34	0.273	1.47	1.62	3.04
48	0.257	1.57	1.54	3.36
57	0.518	1.94	1.51	3.37
60	0.319	1.44	1.36	2.73
71	0.294	1.42	1.57	2.9
UD-802AS				
643	3.44	3.56	0.318	0.335
773	3.54	3.9	0.327	0.323
989	3.02	3.31	0.381	0.397
1053	3.48	3.63	0.426	0.444
1081	3.45	3.82	0.391	0.424
1129	2.96	3.71	0.397	0.392
1262	3.15	3.6	0.394	0.409
1367	3.29	3.61	0.407	0.399
Background				
UD-809AS				
14	0.0123	0.0244	0.0255	0.0264
30	0.0156	0.028	0.0216	0.0236

ID Number	Element 1	Element 2	Element 3	Element 4
UD-802AS				
746	0.0515	0.047	0.0023	0.0031
1006	0.0416	0.048	0.0043	0.0044

Table A.4.3 TLD Readings in Units of R^* for Dosimeters Exposed to 5 rem (0.484 rad) of D_2O-Moderated ^{252}Cf.

ID Number	Element 1	Element 2	Element 3	Element 4
UD-809AS				
15	0.671	3.28	3.51	7.01
19	0.708	3.94	4.16	9.08
23	0.639	3.38	4.05	7.66
34	0.706	3.88	4.19	7.81
48	0.591	3.72	3.79	8.36
57	0.933	4.26	3.7	8.67
60	0.725	3.43	3.22	6.31
71	0.727	3.55	3.9	7.28
UD-802AS				
643	8.4	8.58	0.786	0.827
773	7.54	8.47	0.776	0.762
989	7.8	8.6	0.955	1.02
1053	7.86	8.87	1.04	1.11
1081	9.1	9.69	1	1.05
1129	8.36	10.3	1.02	1
1262	8.06	8.83	0.933	0.967
1367	7.37	8.33	0.992	0.975
Background				
UD-809AS				
14	0.013	0.0222	0.0228	0.0231
30	0.0144	0.0231	0.022	0.0248

ID Number	Element 1	Element 2	Element 3	Element 4
UD-802AS				
746	0.0527	0.0518	0.0018	0.0019
1006	0.0423	0.0552	0.0024	0.0024

Table A.4.4 TLD Readings in Units of R* for Dosimeters Exposed to 10 rem (0.967 rad) of D_2O-Moderated ^{252}Cf.

ID Number	Element 1	Element 2	Element 3	Element 4
UD-809AS				
15	1.45	7.07	7.48	14.4
19	1.42	7.98	8.45	18.1
23	1.2	6.62	8.13	15.8
34	1.4	7.79	8.39	15.8
48	1.17	7.59	7.68	16.9
57	1.75	8.41	7.14	16.4
60	1.45	7.04	6.79	14
71	1.41	7.04	7.7	14.2
UD-802AS				
643	15.1	16.1	1.58	1.66
773	15.9	17.3	1.55	1.52
989	14.8	16.2	2.04	2.18
1053	17.4	19.4	2.44	2.59
1081	19	20.7	2.26	2.41
1129	14.8	18.4	2.14	2.14
1262	16.1	17.7	2.08	2.13
1367	15.7	17.3	2.28	2.19
Background				
UD-809AS				
14	0.0106	0.0183	0.0189	0.0171
30	0.012	0.0249	0.0182	0.0218

ID Number	Element 1	Element 2	Element 3	Element 4
UD-802AS				
746	0.0472	0.0361	0.0008	0.0009
1006	0.0388	0.0472	0.0014	0.0017

Table A.4.5 TLD Readings in Units of R^* for Dosimeters Exposed to 50 rem (4.84 rad) of D_2O-Moderated ^{252}Cf.

ID Number	Element 1	Element 2	Element 3	Element 4
UD-809AS				
15	6.78	33.5	36.5	77.8
19	6.49	36.9	39.5	96
23	5.83	32.1	38.7	83.7
34	6.74	37.6	40.7	85.5
48	5.58	37.3	37.5	88.9
57	7.54	37.7	33.4	86.4
60	7.28	34.8	32.2	73.4
71	7.18	35	37.7	73.5
UD-802AS				
643	87.5	90.8	9.35	10
773	79.4	89.8	8.91	8.93
989	84.7	89	11	11.4
1053	92	100	12.4	12.9
1081	93.3	104	11.7	12.5
1129	70.4	97.2	11.3	11.1
1262	87.5	96.4	11.2	11.5
1367	74.8	84.3	11.6	11.4
Background				
UD-809AS				
14	0.0073	0.0211	0.0195	0.0175
30	0.0132	0.024	0.0176	0.0198

ID Number	Element 1	Element 2	Element 3	Element 4
UD-802AS				
746	0.0593	0.0512	0.0009	0.0011
1006	0.0456	0.0598	0.0015	0.0014

Table A.4.6 TLD Readings in Units of R* for Dosimeters Exposed to 100 rem (9.67 rad) of D_2O-Moderated ^{252}Cf.

ID Number	Element 1	Element 2	Element 3	Element 4
UD-809AS				
15	13.4	73.7	78.9	159
19	13.5	87.8	89.1	201
23	12.1	73.6	87.2	170
34	12.8	80.5	86.8	163
48	10.6	81.6	82	181
57	14.9	83.8	72.3	177
60	14.7	78.4	74	150
71	13.9	76.8	84.4	161
UD-802AS				
643	179	183	20.5	22.3
773	158	177	19	19
989	155	166	22.3	23.4
1053	187	212	27.4	28.9
1081	193	208	23.9	25.5
1129	169	206	23.9	23.5
1262	176	191	23.8	24.4
1367	150	169	24.7	24.5
Background				
UD-809AS				
14	0.0116	0.0232	0.0188	0.0204
30	0.0146	0.0249	0.0213	0.023

ID Number	Element 1	Element 2	Element 3	Element 4
UD-802AS				
746	0.0709	0.0563	0.0013	0.0013
1006	0.0587	0.0765	0.0015	0.0018

Table A.4.7 TLD Readings in Units of R* for Dosimeters Exposed to 499 rem (48.23 rad) of D_2O-Moderated ^{252}Cf.

ID Number	Element 1	Element 2	Element 3	Element 4
UD-809AS				
15	77.6	428	440	864
19	74.4	497	472	1040
21	86.2	487	473	983
42	80	481	466	1000
UD-802AS				
773	906	998	123	123
818	886	1010	137	133
1081	1040	1130	144	153
1311	859	1040	150	130
Background				
UD-809AS				
14	0.0142	0.023	0.0242	0.0241
30	0.0165	0.0298	0.0245	0.025
UD-802AS				
746	0.0958	0.0609	0.0031	0.0034
1006	0.0832	0.0834	0.0035	0.0033

Table A.4.8 TLD Readings in Units of R* for Dosimeters Exposed to 747 rem (72.27 rad) of D_2O-Moderated ^{252}Cf.

ID Number	Element 1	Element 2	Element 3	Element 4
UD-809AS				
48	87	663	632	1370
55	123	650	640	1270
57	122	682	573	1360
60	116	628	559	1150
UD-802AS				
643	1300	1290	-	-
1053	1420	1540	-	-
1100	1190	1220	-	197
1367	1190	1310	-	-
Background				
UD-809AS				
	E1	E2	E3	E4
1806	0.0155	0.0249	0.0319	0.0236
1813	0.0175	0.0222	0.0365	0.0201
UD-802AS				
623	0.0433	0.0458	0.0077	0.0069
962	0.0488	0.0479	0.0074	0.0074

Table A.4.9 TLD Readings in Units of R^* for Dosimeters Exposed to 939 rem (90.80 rad) of D_2O-Moderated ^{252}Cf.

ID Number	Element 1	Element 2	Element 3	Element 4
UD-809AS				
22	161	819	848	1760
23	119	721	819	1570
34	131	812	854	1620
71	141	759	802	1520
UD-802AS				
989	1510	1600	-	-
1112	1690	1700	-	-
1129	1730	2110	-	-
1262	1600	1750	-	-
Background				
UD-809AS				
1802	0.0173	0.0248	0.0226	0.0226
1803	0.016	0.0208	0.0342	0.0228
UD-802AS				
629	0.0369	0.0422	0.0148	0.017
1245	0.0633	0.055	0.0088	0.0103

Table A.4.10 TLD Readings in Units of R* for Dosimeters Exposed to 5,089 rem (492.12 rad) of D_2O-Moderated ^{252}Cf.

ID Number	Element 1	Element 2	Element 3	Element 4
UD-809AS				
22	1030	4630	5070	8080
42	854	4020	4550	7350
57	1020	4590	3990	6650
UD-802AS				
818	4230	4720	360	370
1367	4430	4660	369	368
Background				
UD-809AS				
32	0.007	0.0096	0.0084	0.0106
1806	0.0032	0.0049	0.0002	0.0002
UD-802AS				
623	0.0057	0.0066	0.0032	0.0032
1471	0.0072	0.0079	0.0038	0.0039

Table A.4.11 TLD Readings in Units of R* for Dosimeters Exposed to 7,756 rem (750.0 rad) of D_2O-Moderated ^{252}Cf.

ID Number	Element 1	Element 2	Element 3	Element 4
UD-809AS				
19	1210	6170	6620	9810
23	1490	6330	6940	9140
60	1680	6340	5970	8330
71	1310	5840	6450	9190
UD-802AS				
643	7150	7060	486	486
989	6140	6630	407	414
1081	5210	5840	420	427
1129	6240	7050	398	395
Background				
UD-809AS				
62	0.0055	0.0128	0.0071	0.0086
1801	0.0041	0.0048	0.0002	0.0001
1804	0.0036	0.0061	0.0002	0.0001
UD-802AS				
920	0.0063	0.0068	0.0052	0.0056
1028	0.0113	0.0085	0.0086	0.0074
1359	0.0106	0.0081	0.0064	0.0065

Table A.4.12 TLD Readings in Units of R* for Dosimeters Exposed to 10,611 rem (1026.09 rad) of D_2O-Moderated ^{252}Cf.

ID Number	Element 1	Element 2	Element 3	Element 4
UD-809AS				
15	2040	7420	8110	10900
22	2740	8570	8760	11500
42	1810	7460	7950	10800
57	2470	8830	8530	11000
UD-802AS				
773	6470	7140	443	449
818	6640	7190	415	423
1112	8170	8100	432	432
1367	6300	6540	420	419
Background				
UD-809AS				
32	0.0126	0.0139	0.0155	0.0202
1806	0.0091	0.0085	0.0003	0.0003
UD-802AS				
623	0.0155	0.0109	0.0096	0.0089
1471	0.016	0.0133	0.0129	0.0116

A.5 Data for Phantom Effects

Table A.5.1 TLD Readings in Units of mR* for Dosimeters Exposed to 500 mrem of D_2O-Moderated ^{252}Cf at 50 cm in Air.

ID Number	Element 1	Element 2	Element 3	Element 4
UD-809AS				
40	49.2	284	245	256
51	51.9	202	204	212
1805	46.4	206	229	234
1812	48.3	194	187	207
UD-802AS				
701	181	196	64.4	67.9
770	168	175	58	56.3
838	195	194	75.4	61.5
1079	190	203	81.5	81.2
Background				
UD-809AS				
26	10	11.7	11.7	13.3
63	6.7	15.5	10.5	12.3
1811	6.9	17.2	16	11.6
UD-802AS				
742	28.8	26	1.2	1.1
774	11.3	7.9	0.9	1
1469	25.1	22.9	1.4	1.2

Table A.5.2 TLD Readings in Units of mR* for Dosimeters Exposed to 500 mrem of Bare ^{252}Cf at 50 cm in Air.

ID Number	Element 1	Element 2	Element 3	Element 4
UD-809AS				
10	24.4	31.6	33.4	31
53	20.2	33.6	25.6	35.2
1802	18.4	27.7	26.5	23.7
1810	19.4	23.1	23.6	23.7
UD-802AS				
1192	60.8	52.9	26	25.3
1254	60.5	59.6	27.6	27.1
1468	68.6	62.1	28.7	27.5
1474	64.4	59.9	28	27.9

Table A.5.3 TLD Readings in Units of mR* for Dosimeters Exposed to 500 mrem of Polyethylene-Moderated ^{252}Cf at 50 cm in Air.

ID Number	Element 1	Element 2	Element 3	Element 4
UD-809AS				
33	132	639	585	218
35	117	682	217	231
44	134	633	216	218
50	118	488	200	192
UD-802AS				
855	701	669	236	194
1110	899	655	205	183
1125	836	830	241	195
1255	690	621	218	193

APPENDIX B

VENDOR'S ADDRESSES AND TELEPHONE NUMBERS

AMERSHAM CORPORATION
2636 South Clearbrook Drive
Arlington Heights, IL 60005
Phone: (800) 323-6695

J. L. SHEPHERD and Associates
1010 Arroyo Avenue
San Fernado, CA 91340
Phone: (818) 898-2361

Panasonic Industrial Company
Two Panasonic Way
Secaucus, NJ 07094
Phone: (201) 348-5200

PANTAK, INC.
31 Business Park
Branford, CT 06405
Phone: (203) 488-7318

APPENDIX C

RESPONSE OF $^{6}Li_{2}{}^{10}B_{4}O_{7}$ TO ROOM SCATTER

ORNL's Radiation Calibration Laboratory strives to maintain NIST's requirements as a secondary calibration laboratory. Partial requirements include characterizing the neutron fields for air and room scatter. This characterization is very important when calibrating neutron instruments because the instruments not only detect the direct radiation from the source but also the scattered neutrons from air and the walls of the exposure room. If one does not correct for room and air scatter, the instruments often will over-respond. This is particularly true for instruments that detect thermal neutrons. The scattering of neutrons in air and off the walls of the exposure room cause neutrons to be moderated or slowed down which not only leads to a higher neutron fluence than the direct radiation being detected but also an over-response in some thermal neutron detectors. This is believed to be the case for the Panasonic's albedo dosimeter, UD-809AS, which uses $^{6}Li_{2}{}^{10}B_{4}O_{7}$.

There are two basic techniques being considered for characterizing room return and air scattering: the shadow-cone technique and a polynomial technique. The shadow-cone technique employs a shadow-cone which blocks the direct radiation from the source to the detector so that only the scattered radiation is detected. However, the shape of the shadow-cone should match the source-detector geometry which implies that specific

shadow cones must be designed and constructed to match each detector (Eisenhauer, Schwartz, and Hunt, 1985). Also, the shadow-cone technique is generally recommended for larger rooms (Schwartz, 1993). Because RADCAL's neutron room is relatively small (9.1 x 9.1 x 5.8 m) and because an extensive shadow-cone set would have to be constructed, the polynomial technique is used.

The polynomial technique considers that a neutron instrument not only responds to direct radiation, but also to air and room scatter. As seen by Equation A.1, the assumption is made that room scatter is basically constant and that air scatter is inversely proportional to the distance.

$$D = \frac{Q\sigma_0}{4\pi r^2}(1 + Ar + Sr^2) \qquad (C.1)$$

where D = total detector response,

Q = source emission rate,

r = distance from source to the detector,

σ_0 = response per unit fluence of source neutrons,

Ar = relative response to air scatter, and

Sr^2 = relative response to room scatter neutrons

(Eisenhauer, Schwartz, and McCall, 1987). Because air scatter only shows a relatively small increase in neutron detectors' responses (Schwartz and Eisenhauer, 1982), the air scatter component in Equation A.1 is dropped for simplification. A simplified version of the total detector's response is found in Equation A.2.

A more accurate total response for calibration purposes should include air scatter which

$$D = \frac{Q\sigma_0}{4\pi r^2}(1 + Sr^2) \qquad (C.2)$$

can be calculated using Monte Carlo. Further simplification is useful for the direct contribution (D_0) which is found in Equation A.3.

$$D_0 = \frac{Q\sigma_0}{4\pi} \qquad (C.3)$$

By substituting direct contribution into Equation A.2, the total response becomes Equation A.4.

$$D = \frac{D_0}{r^2}(1 + Sr^2) \qquad (C.4)$$

Equation A.4 can also be written in the following form:

$$Dr^2 = D_0(1 + Sr^2) \qquad (C.5)$$

Thus, by plotting a detector's response (D) at different distances (r) and by fitting a regression line in the form of distance squared (r^2) versus response times distance squared ($D \times r^2$), the direct response at one meter (D_0) and the fractional room return at one meter (S) can be found (Schwartz and Eisenhauer, 1982).

The polynomial technique is used in calculating the response of $^6Li_2{}^{10}B_4O_7$ to room scatter and uses a Bonner sphere set which includes a 2", 3", 5", 8", 10", and a 12" spheres in a 4 x 4 mm LiI detector. Measurements for each sphere are made from 0.5 m to 2.89 m. The fractional room return and the direct response at one meter are found for each sphere using the polynomial technique for the following neutron sources: bare and D_2O-moderated ^{252}Cf. Resulting graphs are found in Figures C.1 - C.7 for bare ^{252}Cf

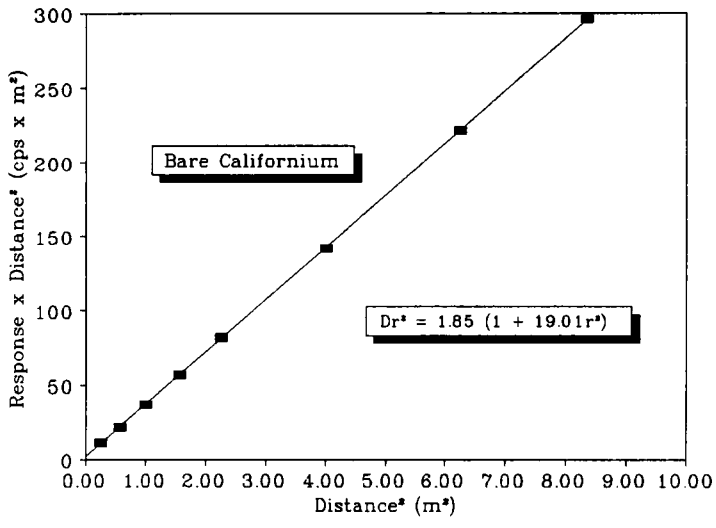


Figure C.1 Response of Bare Detector as a Function of Distance^2 for Bare ^{252}Cf.

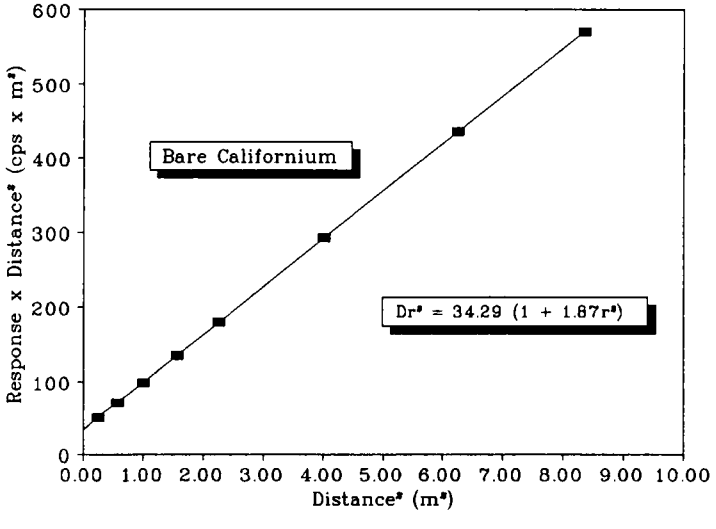


Figure C.2 Response of Two Inch Sphere Detector as a Function of Distance^2 for Bare ^{252}Cf.

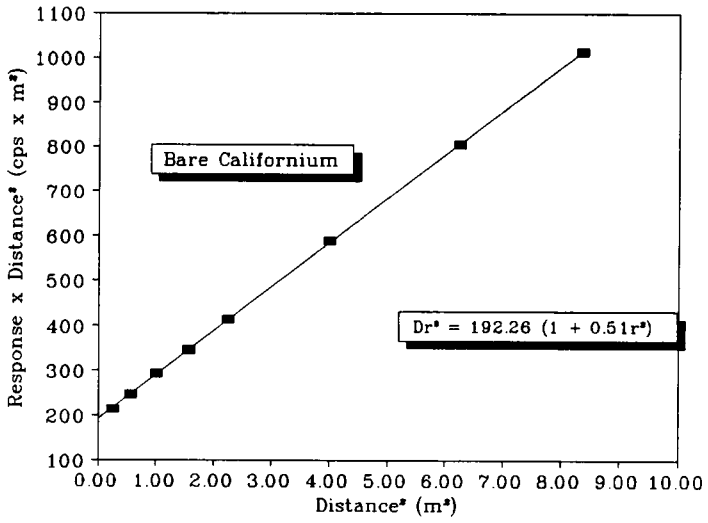


Figure C.3 Response of Three Inch Sphere Detector as a Function of Distance^2 for Bare ^{252}Cf.

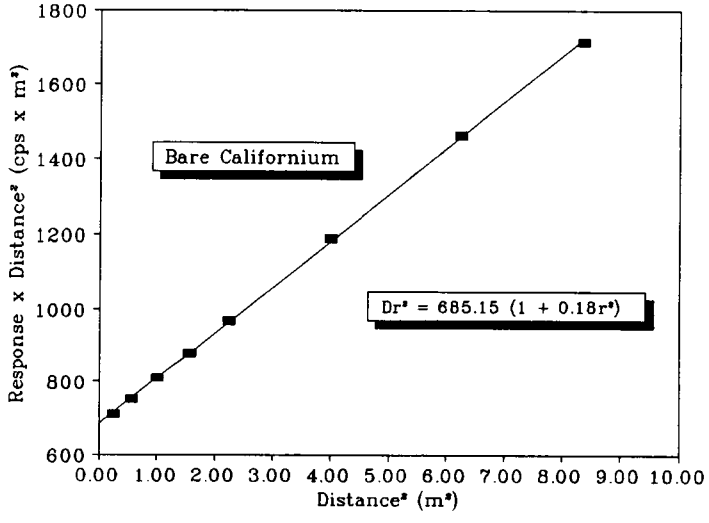


Figure C.4 Response of Five Inch Sphere Detector as a Function of Distance^2 for Bare ^{252}Cf.

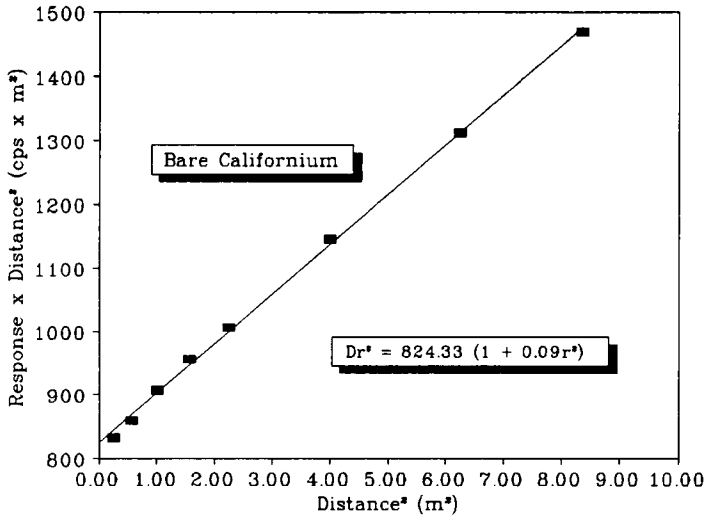


Figure C.5 Response of Eight Inch Sphere Detector as a Function of Distance^2 for Bare ^{252}Cf.

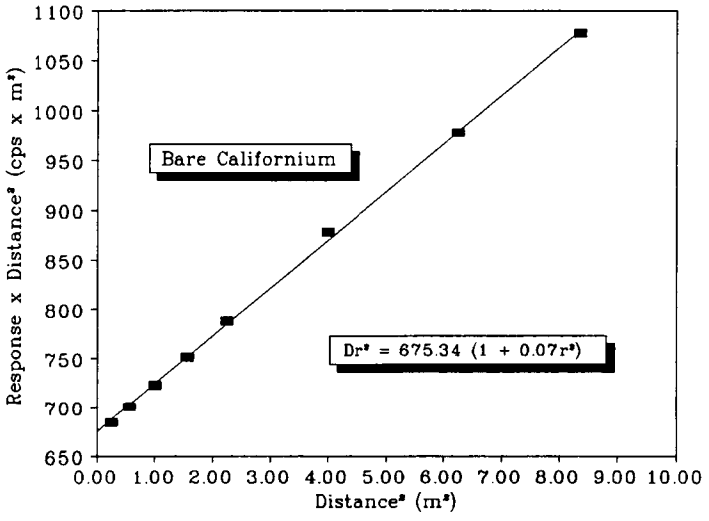


Figure C.6 Response of Ten Inch Sphere Detector as a Function of Distance^2 for Bare ^{252}Cf.

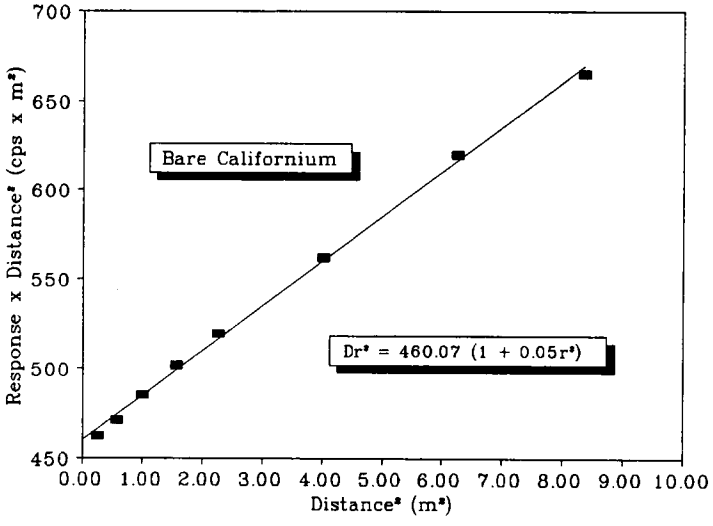


Figure C.7 Response of Twelve Inch Sphere Detector as a Function of Distance^2 for Bare ^{252}Cf.

and in Figures C.8 - C.14 for D_2O-moderated ^{252}Cf. The room return and the direct contribution can then be used in SPUN2, a multisphere unfolding code that calculates the fluence, dose, and dose equivalent as a function of neutron energy (Brackenbush and Scherpelz, 1988). The version of SPUN2 being used has been modified from its original FORTRAN to Quick Basic to include forty-eight energy bins, perspective spectrum, and response data from the IAEA (IAEA 318, 1990).

The direct contribution at one meter for each sphere and source is the Y-intercept from each graph. The direct plus scattered contribution is the actual measurement at one meter. SPUN2 is run once using the direct contribution and then again using the direct plus scattered contribution for each source. SPUN2 not only gives a total flux, but also the flux in each energy bin. An overall scattered flux can be found by using the output from the direct and direct plus scattered fluxes as seen by Equation A.6.

$$\%\,\text{Scattered Flux} = \frac{\text{Flux}_{\text{Dir + Scat}} - \text{Flux}_{\text{Dir}}}{\text{Flux}_{\text{Dir}}} \qquad \text{(C.6)}$$

The overall scattered Flux for bare ^{252}Cf is 24.1% and for D_2O-moderated ^{252}Cf is 20.5%.

The response of the Panasonic UD-809AS to room scatter is found by taking the flux (n/cm^2 s) in each energy bin for direct and direct plus scattered and multiplying by the corresponding response of the dosimeter (rad ^{137}Cs / n/cm^2). The resulting graphs (A.15 and A.16) show that for D_2O-moderated ^{252}Cf there is a distinct over-response to room scatter in the thermal region but a smaller over-response for bare ^{252}Cf.

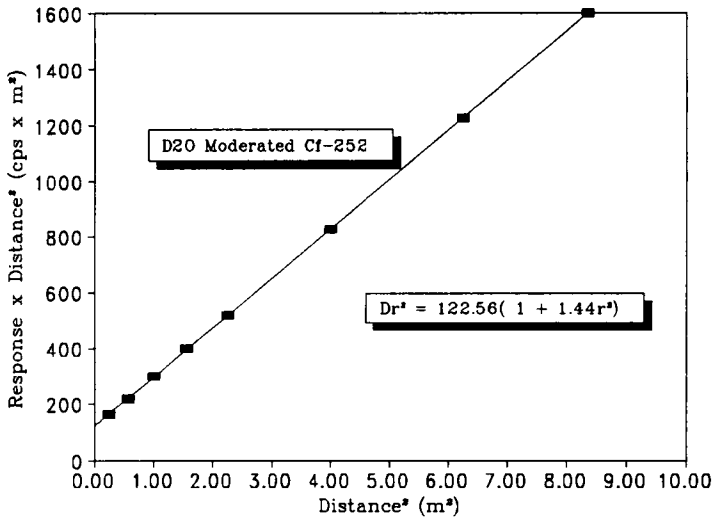


Figure C.8 Response of Bare Detector as a Function of Distance^2 for D_2O-Moderated ^{252}Cf.

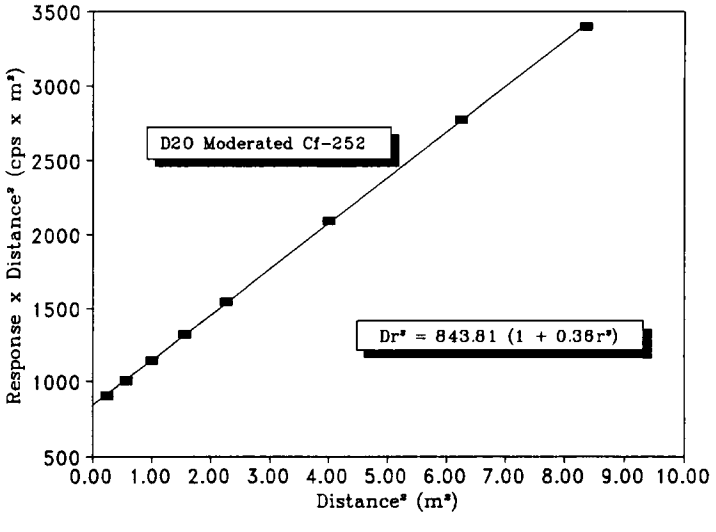


Figure C.9 Response of Two Inch Sphere Detector as a Function of Distance^2 for D_2O-Moderated ^{252}Cf.

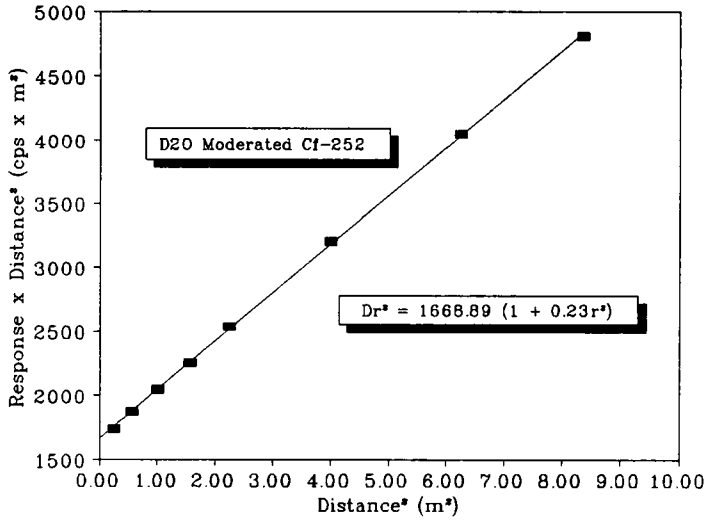


Figure C.10 Response of Three Inch Sphere Detector as a Function of Distance^2 for D_2O-Moderated ^{252}Cf.

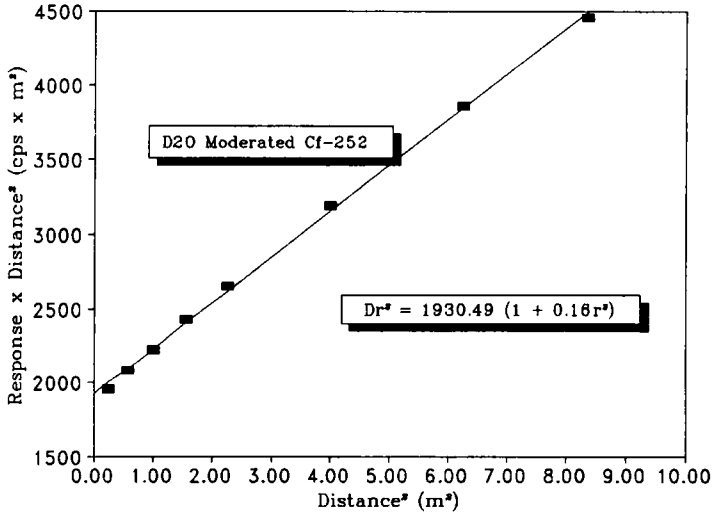


Figure C.11 Response of Five Inch Sphere Detector as a Function of Distance^2 for D_2O-Moderated ^{252}Cf.

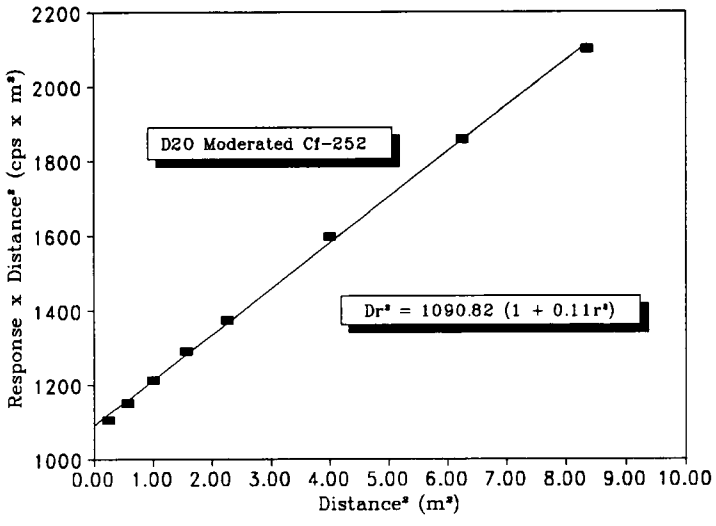


Figure C.12 Response of Eight Inch Sphere Detector as a Function of Distance^2 for D_2O-Moderated ^{252}Cf.

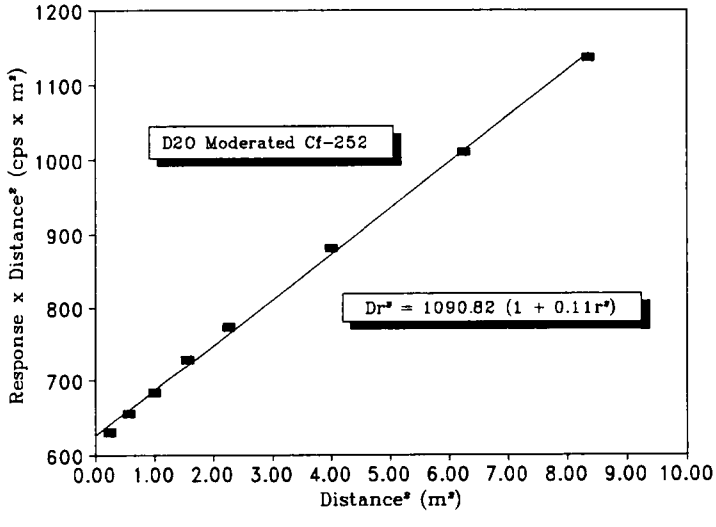


Figure C.13 Response of Ten Inch Sphere Detector as a Function of Distance^2 for D_2O-Moderated ^{252}Cf.

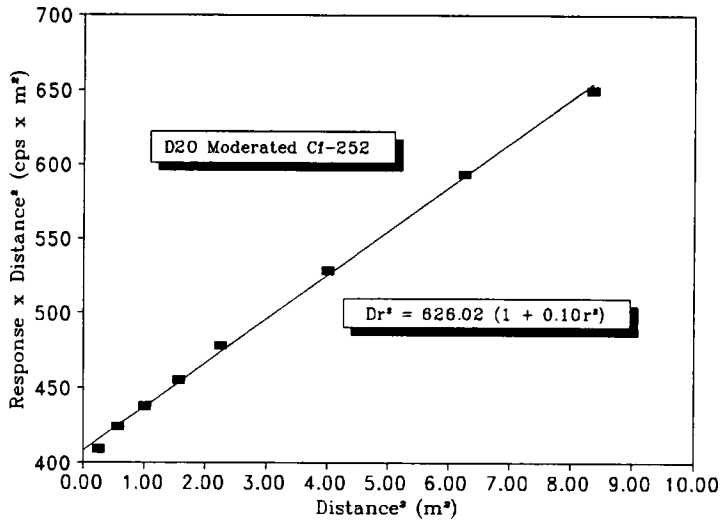


Figure C.14 Response of Twelve Inch Sphere Detector as a Function of Distance^2 for D_2O-Moderated ^{252}Cf.

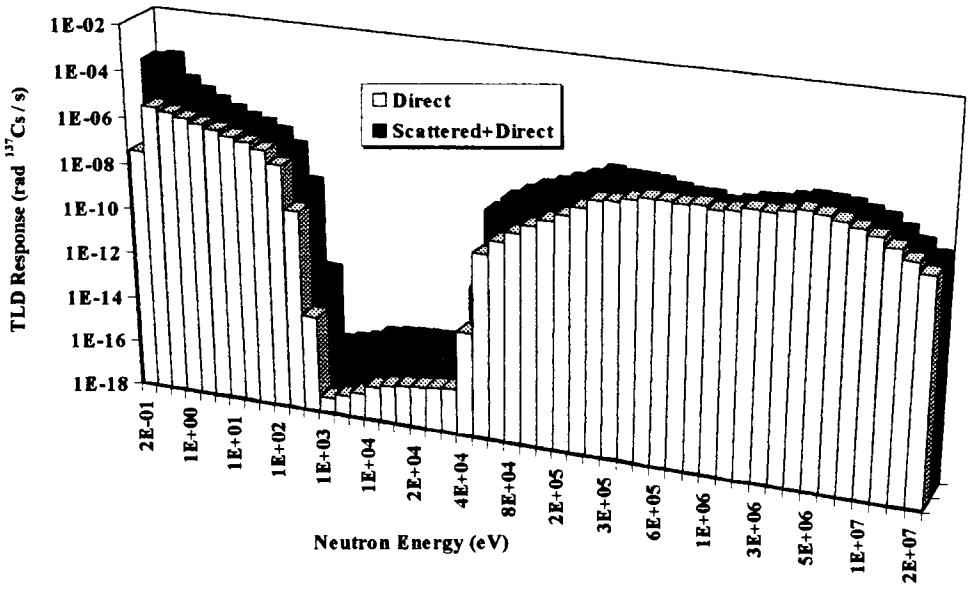


Figure C.15 Response of $^{6}Li_{2}{}^{10}B_{4}O_{7}$ to Direct and Room Scatter Flux for Bare ^{252}Cf.

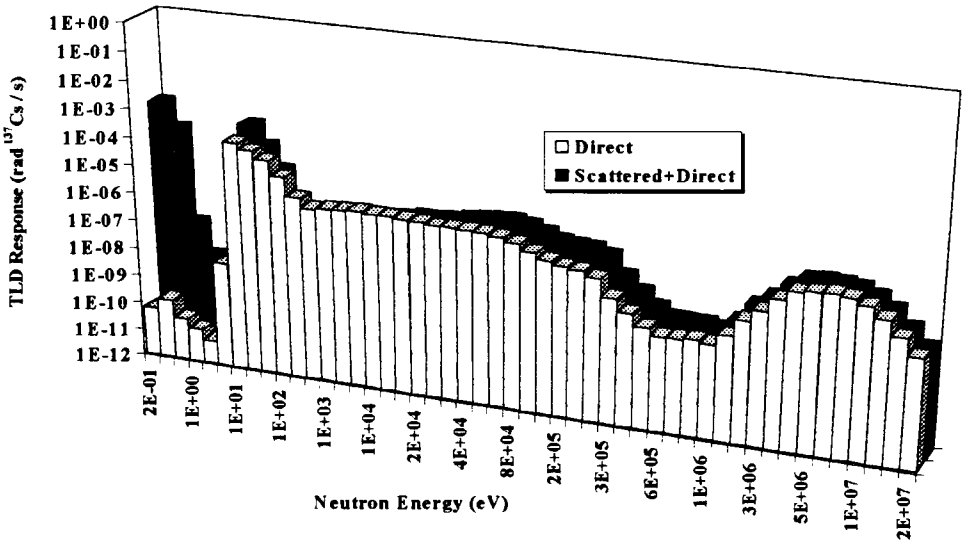


Figure C.16 Response of $^{6}Li_2{}^{10}B_4O_7$ to Direct and Room Scatter Flux for D_2O-Moderated ^{252}Cf.

VITA

Eugenia Beth Lee was born in Knoxville, Tennessee on July 30, 1970. She grew up and attended school in Sevier County, Tennessee. After graduating from Sevier County High School in June of 1988, she began Carson-Newman College the next fall. In May of 1992, Eugenia received a Bachelor of Arts degree in physics from Carson-Newman College. During the fall of 1992, she enrolled at the University of Tennessee, Knoxville. Eugenia received a Master Science degree in Nuclear Engineering with a concentration in Radiation Protection.